What Is the Optimal Activity Coefficient Model To Be Combined with the translated–consistent Peng–Robinson Equation of State through Advanced Mixing Rules? Cross-Comparison and Grading of the Wilson, UNIQUAC, and NRTL aE Models against a Benchmark Database Involving 200 Binary Systems

Andrés Piña-Martinez, Romain Privat, Ilias K Nikolaidis, Ioannis G Economou, Jean-Noël Jaubert

I&EC research
Industrial & Engineering Chemistry Research

pubs.acs.org/IECR

Article

What Is the Optimal Activity Coefficient Model To Be Combined with the *translated–consistent* Peng–Robinson Equation of State through Advanced Mixing Rules? Cross-Comparison and Grading of the Wilson, UNIQUAC, and NRTL a^E Models against a Benchmark Database Involving 200 Binary Systems

Andrés Piña-Martinez, Romain Privat,* Ilias K. Nikolaidis, Ioannis G. Economou,* and Jean-Noël Jaubert*

Cite This: *Ind. Eng. Chem. Res.* 2021, 60, 17228–17247

Read Online

ACCESS | Metrics & More | Article Recommendations | Supporting Information

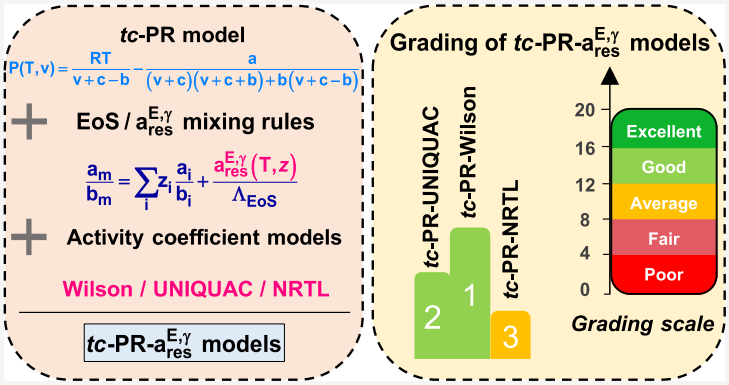

ABSTRACT: The extension of the *translated–consistent* Peng–Robinson (*tc*-PR) equation of state (EoS) to mixtures has been investigated. For this purpose, advanced EoS/$a_{res}^{E,\gamma}$ mixing rules are used to combine the *tc*-PR EoS with the residual part of an activity coefficient model chosen among the Wilson, nonrandom two-liquid (NRTL), and universal quasi-chemical (UNIQUAC) models. The performances of the three resulting EoS versions are compared against a high-quality reference database containing binary system data, specifically selected for the cross-comparison of thermodynamic models and the assessment of their accuracy. It is shown that the best choice to extend the *tc*-PR EoS to mixtures along with EoS/$a_{res}^{E,\gamma}$ mixing rules is to use the residual part of the Wilson activity coefficient model ($a_{res}^{E,Wilson}$). After grading, the resulting model, named "*tc*-PR-Wilson", received a mark of 12.4/20. It has a clear advantage over the other investigated models in this study, which all have marks below 12/20. Observing that some experimental data could not be compared to a calculated value (typically, when the model does not predict the right topology of a phase diagram such as, e.g., predicting a heterogeneous azeotrope instead of a homogeneous one), a new performance indicator ("success ratio") was introduced as the ratio of the number of data points for which the model can reproduce qualitatively the experimental data behavior over the total number of experimental data. The success ratio of the *tc*-PR-Wilson model reaches 0.96; this model outperforms especially in the correlation of liquid- and gas-phase compositions, azeotropic points, and three-phase pressures.

1. INTRODUCTION

Phase-equilibrium thermodynamics is one of the cornerstones of computer-aided process design. The availability of accurate thermodynamic models, capable of estimating saturation and caloric properties, is crucial and necessary to understand and obtain reliable designs of unit operations such as distillation, absorption, extraction, adsorption, and leaching, which are essential unit operations in the chemical industry.

Equations of state (EoSs) are developed with the aim to increase their range of applicability (in terms of the mixture type, composition, temperature and pressure conditions) and to improve the accuracy of mass and energy balances that are necessary for the design of chemical processes. The develop-

Received: July 27, 2021
Revised: September 29, 2021
Accepted: October 20, 2021
Published: November 18, 2021

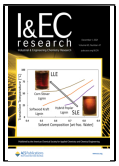

https://doi.org/10.1021/acs.iecr.1c03003
Ind. Eng. Chem. Res. 2021, 60, 17228–17247

ment of the EoS can be divided into two stages: (1) the formulation of a model for pure components and (2) its extension to mixtures. In both stages, a key point is the parameterization, that is, the allocation of numerical values to component-dependent parameters.

With the aim of developing a reliable and accurate EoS for process and product design, Le Guennec et al.[1] introduced the pure-component *translated–consistent* Peng–Robinson (*tc*-PR) cubic equation of state (CEoS)

$$P(T,v) = \frac{RT}{v + c_i - b_i} - \frac{a_i(T)}{(v + c_i)(v + c_i + b_i) + b_i(v + c_i - b_i)}$$

$$\text{with} \begin{cases} a_i(T) = a_{c,i}\cdot\alpha_i(T_r); \qquad T_r = \dfrac{T}{T_{c,i,\exp}} \\ \alpha_i(T_r) = T_r^{N_i(M_i-1)} \exp[L_i(1 - T_r^{M_iN_i})] \\ c_i = v_{i,\mathrm{liq}}^{\mathrm{sat,u\text{-}PR}}(T_r = 0.8) - v_{i,\mathrm{liq,exp}}^{\mathrm{sat}}(T_r = 0.8) \\ \eta_c = [1 + \sqrt[3]{4 - 2\sqrt{2}} + \sqrt[3]{4 + 2\sqrt{2}}\,]^{-1} \approx 0.25308 \\ a_{c,i} = \dfrac{40\eta_c + 8}{49 - 37\eta_c}\dfrac{R^2T_{c,i,\exp}^2}{P_{c,i,\exp}} \approx 0.45724\dfrac{R^2T_{c,i,\exp}^2}{P_{c,i,\exp}} \\ b_i = \dfrac{\eta_c}{\eta_c + 3}\dfrac{RT_{c,i,\exp}}{P_{c,i,\exp}} \approx 0.07780\dfrac{RT_{c,i,\exp}}{P_{c,i\exp}} \end{cases} \tag{1}$$

Table 1. Parameters r_1 and r_2 for Some Classical CEoSs

equation	r_1	r_2
van der Waals[11]	0	0
Redlich–Kwong[12]	−1	0
Peng–Robinson[13]	$-1 - \sqrt{2}$	$-1 + \sqrt{2}$

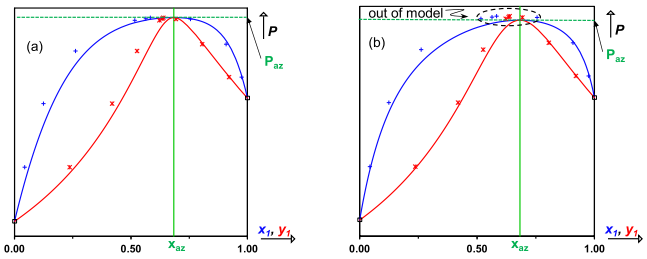

Figure 1. (a) Calculated and experimental isothermal pressure—composition VLE phase diagram that does not exhibit *out-of-model* points. (b) Phase diagrams exhibiting *out-of-model* points due to an underestimation of the experimental azeotropic pressure by the model. (Red *): experimental dew points. (Blue +): experimental bubble points. (Red −): calculated dew curve. (Blue −): calculated bubble curve. P_{az}: calculated azeotropic pressure. x_{az}: calculated azeotropic composition.

In eq 1, the attractive term $a_i(T)$ is classically expressed as the product of its value at the critical temperature ($a_{c,i}$) and the so-called α-function. The covolume, that is, the molar volume when the pressure tends to infinity (here denoted v_i^∞) is related to parameter b_i through $v_i^\infty = b_i - c_i$. Such a model is called *translated*[2,3] because the substance-dependent volume-translation parameter, c_i, is determined, component by component, in order that the translated EoS exactly reproduces the experimental saturated liquid volume at a reduced temperature of 0.8, $[v_{i,\mathrm{liq,exp}}^{\mathrm{sat}}(T_r = 0.8)]$, that is

$$c_i = v_{i,\mathrm{liq}}^{\mathrm{sat,u\text{-}CEoS}}(T_r = 0.8) - v_{i,\mathrm{liq,exp}}^{\mathrm{sat}}(T_r = 0.8) \tag{2}$$

where $v_{i,\mathrm{liq}}^{\mathrm{sat,u\text{-}CEoS}}(T_r = 0.8)$ is the molar volume calculated with the original (*untranslated*) CEoS at $T_r = 0.8$. In turn, *consistent* stands for the fact that the *tc*-PR EoS relies on an α-function that passed the *consistency test* proposed by Le Guennec et al.[4,5] Such a test is made up of a list of constraints that an α-function should absolutely fulfill to guarantee safe property predictions in both subcritical and supercritical domains. These constraints are given in eq 3.

For any reduced temperature (T_r)

$$: \begin{cases} \alpha(T_r) \geq 0 \text{ and } \alpha \text{ continuous} \\ \dfrac{\mathrm{d}\alpha}{\mathrm{d}T_r}(T_r) \leq 0 \text{ and } \dfrac{\mathrm{d}\alpha}{\mathrm{d}T_r} \text{ continuous} \\ \dfrac{\mathrm{d}^2\alpha}{\mathrm{d}T_r^2}(T_r) \geq 0 \text{ and } \dfrac{\mathrm{d}^2\alpha}{\mathrm{d}T_r^2} \text{ continuous} \\ \dfrac{\mathrm{d}^3\alpha}{\mathrm{d}T_r^3}(T_r) \leq 0 \end{cases} \tag{3}$$

As shown in eq 1, the *tc*-PR EoS is coupled with the highly flexible three-parameter α-function proposed by Twu et al. in 1991.[6] Indeed, such an α-function becomes consistent (satisfies eq 3) if the three L, M, and N parameters are determined under constraints following the procedure proposed by Pina-Martinez et al.[7] The triplets of (L_i, M_i, N_i) consistent parameters with the corresponding volume-translation parameter c_i were recently determined and published for 1800 pure compounds i.[8]

In addition to the two well-defined physical properties ($T_{c,i,\exp}$, $P_{c,i,\exp}$), the *tc*-PR model requires four parameters (L_i, M_i, N_i, c_i) for a given pure compound i. It is an extremely accurate CEoS for pure components since it yields an average overall deviation lower than 2% over the 306 700 pseudoexperimental data points available in the pure compound database that Pina-Martinez et al.[8] proposed to use in order to cross-compare the ability of EoS in the property estimation of pure species. In view of such a low deviation, it is possible to conclude that the first stage of development of the *tc*-PR EoS, that concerns pure components only, is completed. Therefore, the next step should be to extend the EoS to mixtures.

Extension to mixtures requires mixing rules (MRs), and a classical choice is the use of the so-called van der Waals one-fluid (VdW1f) MRs. Other options are related to the use of advanced EoS/$g^{\mathrm{E},\gamma}$ or Wong–Sandler (EoS/$a^{\mathrm{E},\gamma}$) MRs. In this work, advanced MRs (EoS/$a_{\mathrm{res}}^{\mathrm{E},\gamma}$) derived by equating the residual part of the excess Helmholtz energy from an EoS and from an explicit activity coefficient model (ACM) are retained. The research objective is to determine which ACM among the Wilson, universal quasi-chemical (UNIQUAC), and non-random two-liquid (NRTL) models is the most suitable to extend the *tc*-PR EoS to mixtures using EoS/$a_{\mathrm{res}}^{\mathrm{E},\gamma}$ MRs. For this purpose, it is decided to use the high-quality reference database developed by the authors.[9] Such a database contains binary system data specifically selected for the cross-comparison of thermodynamic models and the assessment of their accuracy. Models such as the PR EoS incorporating classical MRs and temperature-dependent binary interaction parameters (BIPs) and the PC-SAFT EoS with no association term and no

https://doi.org/10.1021/acs.iecr.1c03003
Ind. Eng. Chem. Res. 2021, 60, 17228−17247

Table 2. Final Marks and Corresponding Success Ratios of the *tc*-PR-Wilson, *tc*-PR-UNIQUAC, *tc*-PR-NRTL, and PR−Van Laar Models Using the Grading Procedure Described by Jaubert et al.[9] and Updated as Described in Section 3.1[a]

		success ratios[b]					
model	final mark (over 20)	overall[c]	*x*	*y*	LLV	Crit	Az
tc-PR-Wilson	12.4	0.96	0.95	0.94	0.83	0.96	0.97
tc-PR-UNIQUAC	11.8	0.97	0.96	0.95	0.79	0.94	0.87
tc-PR-NRTL	11.4	0.96	0.94	0.94	0.77	0.96	0.86
PR−Van Laar	11.5	0.95	0.93	0.93	0.82	0.93	0.72

[a] *x*: liquid-phase composition data (x_1 or x_1^{α}). *y*: gas-phase (or second liquid-phase) composition data (y_1 or x_1^{β}). LLV: three-phase line data. Crit: critical-point data. Az: azeotropic data. [b] Out-of-model data points do not occur for enthalpy and heat capacity of mixing data because it is always possible to calculate these properties at specified *T*, *P*, and z_1 values. [c] The calculation of the overall success ratio includes the h^M and c_P^M data for which such ratios are equal to 1.

regressed BIPs have already been graded against this reference database.[9,10]

This paper is organized in two sections. In Section 2, the implementation of the *tc*-PR model coupled with EoS/$a_{res}^{E,\gamma}$ MRs is introduced. This includes a detailed description of the EoS/$a_{res}^{E,\gamma}$ MRs investigated in this work along with the corresponding ACMs. In Section 3, the performances of the three *tc*-PR-$a_{res}^{E,\gamma}$ models are studied. First, a slight modification of the grading procedure presented by Jaubert et al.[9] and applied to various EoSs previously is briefly summarized. Finally, the results of the grading procedure for the models examined here are discussed.

2. IMPLEMENTATION OF THE *tc*-PR MODEL COUPLED WITH EoS/$a_{RES}^{E,\gamma}$ MIXING RULES

As stated before, this work aims to extend the *tc*-PR model to mixtures using EoS/$a_{res}^{E,\gamma}$ MRs, derived by equaling the residual part of the excess Helmholtz energy from an EoS ($a_{res}^{E,EoS}$) on one side to the same quantity stemming from an explicit ACM (this quantity is denoted $a_{res}^{E,\gamma}$). Three ACMs were tested: the residual part of the Wilson and UNIQUAC models and the purely residual NRTL model. The following part of the present section deals with the introduction of these MRs.

The CEoS can be expressed through the following generic formulation

$$P(T, v, \mathbf{z}) = \frac{RT}{v - b_m} - \frac{a_m}{(v - r_1 b_m)(v - r_2 b_m)} \tag{4}$$

where r_1 and r_2 are two universal constants depending on the selected EoS (see Table 1 for some of the most common CEoSs) and a_m and b_m are the energy (or dispersive, or attractive) and covolume parameters of the mixture, related to the composition of the mixture $\mathbf{z}$ and to the energy $[a_i(T)]$ and covolume (b_i) parameters of the pure components by means of properly defined functions, the so-called MRs.

2.1. Quadratic van der Waals MRs. A popular choice is the so-called VdW1f MRs, which consider parameters a_m and b_m as quadratic functions of the composition

$$\begin{cases} a_m = \sum_i \sum_j z_i z_j a_{ij} & (5) \\ b_m = \sum_i \sum_j z_i z_j b_{ij} & (6) \end{cases}$$

where a_{ij} and b_{ij} are determined from pure-component parameters, a_i and b_i, through the application of combining rules. The classically applied combining rules are the geometric-mean rule for the cross-energy and the arithmetic-mean rule for the cross-covolume parameter:

$$\begin{cases} a_{ij} = \sqrt{a_i a_j}(1 - k_{ij}) & (7) \\ b_{ij} = \frac{b_i + b_j}{2}(1 - l_{ij}) & (8) \end{cases}$$

where k_{ij} and l_{ij} are BIPs, adjustable over experimental data or obtained from suitable correlations.

2.2. EoS/$a_{res}^{E,\gamma}$ MRs. CEoSs with VdW1f MRs lead to very accurate results at low and high pressures for simple mixtures (containing components showing little or no polarity, e.g., hydrocarbons, gases, etc.). However, such MRs cannot be applied with success to polar mixtures. In return, excess Gibbs energy (g^E) models (ACMs) are applicable at low pressures and are able to correlate the phase-equilibrium data for polar mixtures. From this observation arises the idea to combine CEoSs and ACMs in order to obtain a single model suitable for describing the phase equilibria of polar and nonpolar mixtures from low to high pressures. This combination of EoSs and g^E models is possible via the so-called EoS/g^E approach, which is essentially a set of MRs for the energy parameter of CEoSs.[14] The starting point for deriving EoS/g^E models is to equate the expressions of the excess Gibbs energy obtained from an EoS $[g^{E,EoS}(T,P,\mathbf{z})]$ with that from an explicit ACM $[g^{E,\gamma}(T,\mathbf{z})]$. By construction, this latter is temperature- and composition-dependent but pressure-independent; however, the $g^{E,EoS}$ quantity depends on the pressure, temperature, and composition, explaining why a reference pressure, noted P_{ref}, needs to be selected before equating the two quantities. The starting equation to derive EoS/g^E models is thus

$$g^{E,EoS}(T, P_{ref}, \mathbf{z}) = g^{E,\gamma}(T, \mathbf{z}) \tag{9}$$

The ACM may be chosen among the classical forms of molar excess Gibbs energy functions (such as Redlich−Kister, Margules, Wilson, Van Laar, NRTL, UNIQUAC, UNIFAC, and others). Equation 9 is the cornerstone of the approach pioneered by Huron and Vidal (HV),[15] who assumed an infinite reference pressure, and by Michelsen,[16−18] who employed the zero-pressure reference and derived the MHV-1 and MHV-2 MRs.

It is believed that the consistency of eq 9 can be questioned for the following two main observations:

(1) In accordance with the way they were derived, low-pressure $g^{E,\gamma}$ models classically used to calculate the activity coefficients should be better regarded as a^E models (they will be denoted as $a^{E,\gamma}$ hereafter to avoid

https://doi.org/10.1021/acs.iecr.1c03003
Ind. Eng. Chem. Res. 2021, 60, 17228−17247

Table 3. Overview of the MAPEs between the Experimental Data and Model Predictions along with the Corresponding Success Ratios (*tc*-PR-Wilson) for the 200 Binary Systems Included in the Benchmark Database Proposed by Jaubert et al[9,a]

		MAPE and the corresponding success ratio (SR) on														
BAC	type of association	x (%)	SR_x	y (%)	SR_y	P_{LLV} (%)	z_{LLV} (%)	$SR_{PLLV} = SRz_{LLV}$	P_c (%)	x_c (%)	$SR_{P_c} = SR_{x_c}$	P_{az} (%)	x_{az} (%)	$SR_{Paz} = SR_{xaz}$	h^M (%)	c_P^M (%)
1 (NA−NA)	mixtures without association	8.0	0.98	7.6	0.97	3.2	24.6	0.56	7.7	19.0	0.98	0.8	8.1	1.00	34.6	185.3
2 (HA−NA)		10.0	0.95	7.3	0.95	-	-	-	6.0	10.5	0.99	1.7	6.0	1.00	31.4	150.9
3 (HD−NA)		8.6	0.88	6.9	0.88	-	-	-	5.9	17.3	0.98	2.6	6.4	1.00	18.6	155.2
4 (HA−HA or HD−HD)		8.9	0.97	7.6	0.97	-	-	-	5.6	13.7	1.00	15.8	9.9	1.00	24.2	176.3
5 (SA−NA)	mixtures in which self-association tends to be broken	16.2	0.90	25.6	0.91	3.3	29.6	0.84	41.8	57.8	0.98	1.4	8.3	0.97	31.4	104.5
6 (HD−HA)	mixtures in which cross-association takes place alone	8.2	0.96	7.5	0.96	-	-	-	3.1	14.8	1.00	1.5	11.4	1.00	40.3	85.3
7 (SA−HD)	mixtures in which both cross-association and self-association take place	12.6	0.98	10.0	0.98	-	-	-	-	-	-	1.4	7.6	1.00	50.3	64.4
8 (SA−HA)		16.6	0.94	10.7	0.94	1.4	13.1	1.00	19.6	23.9	0.85	1.9	15.1	0.98	42.4	84.1
9 (SA−SA)		21.3	0.94	12.6	0.94	2.7	8.9	1.00	6.3	8.7	0.98	5.5	28.7	0.85	49.4	117.6
overall		**12.5**	**0.95**	**10.3**	**0.94**	**2.7**	**20.3**	**0.83**	**12.6**	**20.8**	**0.96**	**2.7**	**11.8**	**0.97**	**36.9**	**123.4**

[a]The mixtures are classified in nine BACs, as proposed by Jaubert et al.[9] The abbreviations used for the associating character of a pure compound are as follows: NA for "nonassociating", HA for "hydrogen-acceptor", HD for "hydrogen-donor", and SA for "self-associating". Dots (-) indicate that no experimental data are available in the database for the respective properties.

Table 4. Rating of the Nine BACs in Order to Obtain the Final Mark of the *tc*-PR−Wilson Model[a]

		mark on												
BAC	type of association	x	y	P_{LLV}	z_{LLV}	P_c	x_c	P_{az}	x_{az}	h^M	c_P^M	BAC mark	mark (over 20) by type of association	final mark of the *tc*-PR-Wilson model
1 (NA−NA)	mixtures without association	15.7	15.7	10.3	4.3	14.0	10.3	19.6	15.9	11.4	1.5	11.9		
2 (HA−NA)		14.2	15.4	-	-	15.3	14.6	19.2	17.0	12.1	4.9	14.1	$\underbrace{\text{mark}_{NA}}_{\text{non-association}} = 13.2$	
3 (HD−NA)		13.8	14.6	-	-	15.3	11.1	18.7	16.8	15.3	4.5	13.8		
4 (HA−HA or HD−HD)		15.1	15.7	-	-	15.8	13.1	12.1	15.1	13.9	2.4	12.9		
5 (SA−NA)	mixtures in which self-association tends to be broken	10.8	6.5	15.4	4.4	**0.0**	**0.0**	18.7	15.4	12.1	9.6	9.3	$\underbrace{\text{mark}_{SA}}_{\text{self-association}} = 9.3$	**12.4/20**
6 (HD−HA)	mixtures in which cross-association takes place alone	15.3	15.6	-	-	17.6	12.6	19.2	14.3	9.9	11.5	14.5	$\underbrace{\text{mark}_{CA}}_{\text{cross-association}} = 14.5$	
7 (SA−HD)	mixtures in which both cross-association and self-association take place	13.4	14.7	-	-	-	-	19.3	16.2	7.4	13.6	14.1	$\underbrace{\text{mark}_{CA+SA}}_{\text{cross-association +self-association}} = 12.8$	
8 (SA−HA)		11.0	13.7	19.3	13.4	4.5	6.8	18.6	12.1	9.4	11.6	12.1		
9 (SA−SA)		8.8	12.9	18.7	15.6	15.0	15.4	14.6	4.8	7.6	8.2	12.2		
overall mark (eq 35)		**13.0**	**12.8**	**14.9**	**7.7**	**10.6**	**9.0**	**18.2**	**14.2**	**10.9**	**8.9**	**12.4**		

[a]Dots (-) indicate that no experimental data are available in the database for the respective properties.

https://doi.org/10.1021/acs.iecr.1c03003
Ind. Eng. Chem. Res. 2021, 60, 17228−17247

Table 5. Overview of the MAPEs between the Experimental Data and Model Predictions along with the Corresponding Success Ratios (*tc*-PR-UNIQUAC) for the 200 Binary Systems Included in the Benchmark Database Proposed by Jaubert et al[9,a]

	MAPE and the corresponding success ratio (SR) on														
BAC	x (%)	SR_x	y (%)	SR_y	P_{LLV}	z_{LLV}	$SR_{P_{LLV}} = SR_{z_{LLV}}$	P_c (%)	x_c (%)	$SR_{P_c} = SR_{x_c}$	P_{az} (%)	x_{az} (%)	$SR_{P_{az}} = SR_{x_{az}}$	h^M (%)	c_P^M (%)
1 (NA−NA)	10.0	0.99	9.1	0.97	4.1	21.0	0.81	5.7	20.1	0.98	5.7	12.4	1.00	29.7	185.0
2 (HA−NA)	9.9	0.96	7.7	0.96	-	-	-	5.4	11.9	0.98	1.4	5.4	1.00	26.2	160.1
3 (HD−NA)	8.9	0.90	7.1	0.90	-	-	-	5.9	16.3	0.98	2.1	7.9	1.00	16.6	161.3
4 (HA−HA or HD−HD)	10.6	0.96	8.1	0.96	-	-	-	5.5	13.8	1.00	15.0	10.1	1.00	23.1	158.7
5 (SA−NA)	27.6	0.93	28.7	0.94	4.1	30.3	0.56	10.7	58.2	0.89	3.2	7.8	0.71	32.1	168.0
6 (HD−HA)	6.5	0.96	6.3	0.96	-	-	-	2.9	11.5	0.97	1.4	6.5	1.00	22.8	57.3
7 (SA−HD)	32.4	0.97	17.9	0.98	-	-	-	-	-	-	0.7	8.1	0.77	50.9	47.0
8 (SA−HA)	23.2	0.94	12.3	0.94	1.3	14.0	1.00	29.3	24.9	0.77	2.8	20.9	0.76	39.3	120.5
9 (SA−SA)	27.4	0.96	15.5	0.95	2.7	13.1	1.00	6.0	8.7	0.98	6.1	34.3	0.79	42.2	124.7
overall	**16.5**	**0.96**	**11.9**	**0.95**	**3.1**	**19.9**	**0.79**	**9.4**	**21.0**	**0.94**	**3.3**	**13.5**	**0.87**	**32.8**	**136.0**

[a]The mixtures are classified in nine BACs, as proposed by Jaubert et al.[9] The abbreviations used for the associating character of a pure compound are as follows: NA for "nonassociating", HA for "hydrogen-acceptor", HD for "hydrogen-donor" and SA for "self-associating". Dots (-) indicate that no experimental data are available in the database for the respective properties.

Table 6. Rating of the Nine BACs in Order to Obtain the Final Mark of the *tc*-PR-UNIQUAC Model[a]

	mark on												
BAC	x	y	P_{LLV}	z_{LLV}	P_c	x_c	P_{az}	x_{az}	h^M	c_P^M	BAC mark	mark (over 20) by type of association	final mark of the *tc*-PR-UNIQUAC model
1 (NA−NA)	14.8	15.0	14.6	7.7	15.4	9.8	17.2	13.8	12.6	1.5	12.2		
2 (HA−NA)	14.5	15.5	-	-	15.7	13.8	19.3	17.3	13.5	4.0	14.2	$\underbrace{\text{mark}_{NA}}_{\text{non-association}} = 13.3$	
3 (HD−NA)	14.0	14.8	-	-	15.2	11.6	19.0	16.1	15.9	3.9	13.8		
4 (HA−HA or HD−HD)	14.2	15.4	-	-	15.8	13.1	12.5	14.9	14.2	4.1	13.0		
5 (SA−NA)	5.8	5.3	10.1	2.7	10.7	**0.0**	13.2	11.5	12.0	3.2	7.4	$\underbrace{\text{mark}_{SA}}_{\text{self-association}} = 7.4$	**11.8/20**
6 (HD−HA)	16.1	16.2	-	-	17.3	13.8	19.3	16.7	14.3	14.3	16.0	$\underbrace{\text{mark}_{CA}}_{\text{cross-association}} = 16.0$	
7 (SA−HD)	3.7	10.8	-	-	-	-	15.1	12.3	7.3	15.3	10.7		
8 (SA−HA)	7.9	13.0	19.3	13.0	**0.0**	5.8	14.2	7.3	10.2	8.0	9.9	$\underbrace{\text{mark}_{CA+SA}}_{\text{cross-association + self-association}} = 10.6$	
9 (SA−SA)	6.0	11.7	18.7	13.4	15.2	15.3	13.4	2.2	9.5	7.5	11.3		
overall mark (eq 35)	**10.5**	**12.1**	**14.5**	**7.9**	**12.8**	**9.1**	**15.9**	**12.8**	**12.3**	**7.8**	**11.8**		

[a]Dots (-) indicate that no experimental data are available in the database for the respective properties.

https://doi.org/10.1021/acs.iecr.1c03003
Ind. Eng. Chem. Res. 2021, 60, 17228−17247

Table 7. Overview of the MAPEs between the Experimental Data and Model Predictions along with the Corresponding Success Ratios (*tc*-PR-NRTL) for the 200 Binary Systems Included in the Benchmark Database Proposed by Jaubert et al[9,a]

		MAPE and the corresponding success ratio (SR) on													
BAC	x (%)	SR_x	y (%)	SR_y	P_{LLV}(%)	z_{LLV}(%)	$SR_{P_{LLV}} = SR_{z_{LLV}}$	P_c(%)	x_c(%)	$SR_{P_c} = SR_{x_c}$	P_{az}(%)	x_{az}(%)	$SR_{P_{az}} = SR_{x_{az}}$	h^M(%)	c_P^M(%)
1 (NA−NA)	9.9	0.97	8.8	0.96	3.2	14.7	0.75	6.7	20.5	0.97	5.4	8.0	1.00	30.0	184.7
2 (HA−NA)	11.0	0.96	7.9	0.95	-	-	-	3.8	9.3	0.99	1.2	4.3	1.00	28.6	160.0
3 (HD−NA)	8.4	0.90	7.1	0.90	-	-	-	5.8	16.5	0.98	1.9	6.7	1.00	17.5	160.8
4 (HA−HA or HD−HD)	9.9	0.95	7.8	0.95	-	-	-	5.7	12.0	1.00	40.2	20.2	1.00	22.7	158.7
5 (SA−NA)	27.7	0.87	27.3	0.94	12.1	35.8	0.96	13.5	58.5	0.93	3.6	12.9	0.71	31.2	142.3
6 (HD−HA)	6.7	0.96	6.2	0.96	-	-	-	3.2	14.7	1.00	1.2	4.6	0.94	22.6	75.9
7 (SA−HD)	39.6	0.93	20.8	0.94	-	-	-	-	-	-	1.3	10.4	0.69	48.9	95.8
8 (SA−HA)	20.5	0.95	11.8	0.95	2.0	17.3	0.92	22.4	23.1	0.86	1.1	18.4	0.88	39.4	139.8
9 (SA−SA)	22.4	0.91	11.9	0.90	2.4	9.4	0.31	6.2	7.3	0.98	2.7	15.1	0.64	48.7	102.5
overall	**15.6**	**0.94**	**11.2**	**0.94**	**7.1**	**24.8**	**0.77**	**8.7**	**20.3**	**0.96**	**3.5**	**10.9**	**0.86**	**33.9**	**128.3**

[a]The mixtures are classified in nine BACs, as proposed by Jaubert et al.[9] The abbreviations used for the associating character of a pure compound are as follows: NA for "nonassociating", HA for "hydrogen-acceptor", HD for "hydrogen-donor", and SA for "self-associating". Dots (-) indicate that no experimental data are available in the database for the respective properties.

confusion with the same quantity stemming from the EoS);

(2) In eq 9, the combinatorial part and the residual part of g^E stemming from the EoS and from the ACM do not match. Although $g^{E,EoS} = g^{E,\gamma}$, we do not obtain $g^{E,EoS}_{combinatorial} = g^{E,\gamma}_{combinatorial}$ and $g^{E,EoS}_{residual} = g^{E,\gamma}_{residual}$. We can thus expect poor results when athermal or regular solutions that only require a combinatorial or a residual contribution are modeled. To derive MRs, and contrary to eq 9, it is believed that particular attention has to be given separately to the combinatorial and residual contributions. It is advised to equal the combinatorial and residual contributions stemming from the EoS and from the $a^{E,\gamma}$ model separately to ascertain that quantities that contain the same information are equaled.

These two observations led to the modification of the classically used way to derive MRs and resulted in the formulation of EoS/$a^{E,\gamma}_{res}$ MRs that are used in this work. Let us come back to the consequences of the two aforementioned observations for a better understanding of the derivation of EoS/$a^{E,\gamma}_{res}$ MRs.

- As pointed out by Wong and Sandler[19] and also by Jaubert and Privat,[20] observation (1) is supported by the fact that the pressure dependency of ACMs ($g^{E,\gamma}$) is always ignored. Indeed, all excess Gibbs energy models should theoretically depend on pressure, but our current knowledge on liquid theory still lacks accuracy and relies on the incompressible liquid assumption. In consequence, all ACMs predict: $v^{E,\gamma} = -(\partial g^{E,\gamma}/\partial P)_{T,\mathbf{z}} = 0$. Although the experimental values of v^E are often small, such a result is thermodynamically inconsistent (g^E should indeed be a function of the composition, temperature, and pressure) and must be seen as a theoretical weakness. Since $g^{E,\gamma} = a^{E,\gamma} + P{\cdot}v^{E,\gamma}$, the developers of $g^{E,\gamma}$ models (UNIQUAC, Wilson, etc.) decided to construct expressions for $a^{E,\gamma}$ and to use them to determine activity coefficients. As an illustration, in their paper, relative to the derivation of their MRs, Wong and Sandler[19] write: "if one examines the derivation of g^E models, it is evident that it is really a model for a^E which has been derived". In conclusion, all $g^{E,\gamma}$ are in fact $a^{E,\gamma}$ models and some of them, such as NRTL or Van Laar models, that do not contain a combinatorial contribution are even only residual contributions of $a^{E,\gamma}$ models (denoted $a^{E,\gamma}_{res}$). At low pressures, it is reasonable to assume that $g^E \approx a^E$. However, to define the MRs for an EoS potentially used under high pressures, we see no reason to keep such an approximation, and consequently, we propose to derive MRs by equaling the expression of the excess Helmholtz energy from an EoS with the one of a low-pressure $a^{E,\gamma}$ model (rather than equaling excess Gibbs energies). It is exactly what Wong and Sandler[19] made 30 years ago during the development of their MRs under infinite pressure.
- The second observation is a consequence of the natural division of the excess Gibbs energy ($g^E = h^E - Ts^E$) into an enthalpic (or energetic, residual, or regular-solution) and an entropic (or combinatorial or athermal-solution) contribution. A proper modeling of athermal solutions requires an appropriate combinatorial term, whereas an

https://doi.org/10.1021/acs.iecr.1c03003
Ind. Eng. Chem. Res. 2021, 60, 17228−17247

Table 8. Rating of the Nine BACs in Order to Obtain the Final Mark of the *tc*-PR-NRTL Model[a]

	mark on												
BAC	x	y	P_{LLV}	z_{LLV}	P_c	x_c	P_{az}	x_{az}	h^M	c_P^M	BAC mark	mark (over 20) by type of association	final mark of the *tc*-PR-NRTL model
1 (NA−NA)	14.7	15.0	13.8	9.5	14.6	9.5	17.3	16.0	12.5	1.5	12.4		
2 (HA−NA)	13.9	15.3	-	-	16.9	15.1	19.4	17.9	12.8	4.0	14.4	$\underbrace{\text{mark}_{NA}}_{\text{non-association}} = 12.9$	
3 (HD−NA)	14.2	14.8	-	-	15.3	11.5	19.0	16.7	15.6	3.9	13.9		
4 (HA−HA or HD−HD)	14.3	15.3	-	-	15.7	14.0	**0.0**	9.9	14.3	4.1	11.0		
5 (SA−NA)	5.4	6.0	13.4	2.0	9.2	**0.0**	13.0	9.7	12.2	5.8	7.7	$\underbrace{\text{mark}_{SA}}_{\text{self-association}} = 7.7$	**11.4/20**
6 (HD−HA)	16.0	16.3	-	-	17.6	12.6	18.3	16.7	14.3	12.4	15.5	$\underbrace{\text{mark}_{CA}}_{\text{cross-association}} = 15.5$	
7 (SA−HD)	0.2	9.0	-	-	-	-	13.4	10.3	7.8	10.4	8.5		
8 (SA−HA)	9.2	13.4	17.4	10.4	2.8	7.3	17.2	9.5	10.2	6.0	10.3	$\underbrace{\text{mark}_{CA+SA}}_{\text{cross-association +self-association}} = 9.6$	
9 (SA−SA)	8.0	12.7	5.8	4.7	15.1	16.0	11.9	7.9	7.8	9.7	10.0		
overall mark (eq 35)	**10.4**	**12.3**	**12.9**	**6.4**	**12.8**	**9.2**	**14.8**	**12.7**	**12.2**	**7.6**	**11.4**		

[a]Dots (-) indicate that no experimental data are available in the database for the respective properties.

appropriate residual term is required for regular solutions. Each of the combinatorial and residual terms needs to be accurately known for solutions in which deviations from the ideality are the consequence of both enthalpic and entropic effects. It is thus necessary to analyze in detail the features of the combinatorial contributions and residual contributions stemming from an $a^{E,\gamma}$ model and from a CEoS.

Let us start our analysis with the combinatorial contribution and let us see if equating the combinatorial contributions from the EoS and from an $a^{E,\gamma}$ model makes sense. To do so, the following equation is considered

$$a_{comb}^{E,EoS}(T, P, \mathbf{z}) = a_{comb}^{E,\gamma}(T, \mathbf{z}) \tag{10}$$

First, let us recall that the combinatorial contribution to a^E stemming from a CEoS is similar to a Flory−Huggins expression in the form of free volume[21]

$$a_{comb}^{E,EoS}(T, P, \mathbf{z}) = RT\sum_i x_i \ln\left(\frac{v_i - b_i}{v - b_m}\right) \tag{11}$$

On the other hand, the same quantity from an ACM is either zero (Van Laar and NRTL), a Flory−Huggins expression (Wilson), or a Flory−Huggins expression corrected by a Staverman−Guggenheim (SG) term (UNIQUAC)

$$\begin{cases} a_{comb}^{E,NRTL} = a_{comb}^{E,Van\ Laar} = 0 \\ a_{comb}^{E,Wilson} = RT\sum_i x_i \ln\left(\frac{v_i}{v}\right) \\ a_{comb}^{E,UNIQUAC} = RT\sum_i x_i \ln\left(\frac{v_i}{v}\right) + \text{SG term} \end{cases} \tag{12}$$

By comparing eqs 11 and 12, it is clearly impossible to find a MR on b_m so that both equations become identical. We must thus conclude that the CEoS will never be able to reproduce the combinatorial $a_{comb}^{E,\gamma}(T,\mathbf{z})$ expression stemming from an ACM. In other words, we could state that the knowledge of $a_{comb}^{E,\gamma}(T,\mathbf{z})$ is not helpful in deriving MRs, explaining why it is believed that eq 9 is not a suitable starting point. A key point is the acknowledgment of eq 11 to be particularly suitable to describe deviations from the ideality, attributed to the size and shape differences of the components.[22] There is thus no need to constrain the CEoS to reproduce the $a_{comb}^{E,\gamma}(T,\mathbf{z})$ expression. This conclusion is supported also by the observation of the poor correlation of athermal solutions by the MRs obtained by equating (under zero pressure) excess Gibbs energy quantities ($g^{E,EoS}$ and $g^{E,\gamma}$) containing nonidentical combinatorial contributions which, in consequence, do not vanish when equating the two excess quantities. The resulting consequence is the appearance of the well-documented "double-combinatorial term" issue. The reader is here referred to the book by Kontogeorgis and Folas[23] and especially to Section 6.6 for more details.

Let us continue our analysis with the residual contribution and let us see the consequence of writing

$$a_{res}^{E,EoS}(T, P, \mathbf{z}) = a_{res}^{E,\gamma}(T, \mathbf{z}) \tag{13}$$

The residual contribution to a^E stemming from a CEoS is

$$a_{res}^{E,EoS}(T, P, \mathbf{z}) = \sum_i z_i \frac{a_i}{b_i(r_1 - r_2)} \ln\left(\frac{v_i - b_i r_2}{v_i - b_i r_1}\right) - \frac{a_m}{b_m(r_1 - r_2)} \ln\left(\frac{v - b r_2}{v - b r_1}\right) \tag{14}$$

Before equaling such a mathematical relation to $a_{res}^{E,\gamma}(T,\mathbf{z})$, a reference pressure has to be specified. Following the pioneering works of Huron, Vidal, and Michelsen, it is here proposed to successively select $P_{ref} = +\infty$ and $P_{ref} = 0$. The derivations of the corresponding MRs for a_m/b_m at the two considered reference pressures are presented in Appendix A1 of the Supporting Information.

- Case 1: $P_{ref} = +\infty$

By combining eq 13 with eq 14 under infinite pressure, we obtain (the reader is referred to Appendix A1 of the Supporting Information for all the details)

$$\frac{a_m}{b_m} = \sum_i z_i \frac{a_i}{b_i} + \frac{a_{res}^{E,\gamma}(T, \mathbf{z})}{\Lambda_{EoS}}$$
$$\text{with: } \Lambda_{EoS} = \frac{1}{r_2 - r_1} \ln\left(\frac{1 - r_2}{1 - r_1}\right) \tag{15}$$

We can thus state that after selecting freely a MR for the covolume b_m, eq 15 makes it possible to univocally determine a_m.

https://doi.org/10.1021/acs.iecr.1c03003
Ind. Eng. Chem. Res. 2021, 60, 17228−17247

Table 9. Overview of the MAPEs between the Experimental Data and Model Predictions along with the Corresponding Success Ratios (PR–Van Laar) for the 200 Binary Systems Included in the Benchmark Database Proposed by Jaubert et al[9,a]

	MAPE and the corresponding success ratio (SR) on																	
BAC	x (%)	SR_x	y (%)	SR_y	P_{LLV} (%)	z_{LLV} (%)	$SR_{P_{LLV}} = SR_{z_{LLV}}$	P_c (%)	x_c (%)	$SR_{P_c} = SR_{x_c}$	P_{az} (%)	x_{az} (%)	$SR_{P_{az}} = SR_{x_{az}}$	h^M (%)	c_P^M (%)
1 (NA–NA)	7.9	0.97	7.9	0.96	1.3	19.3	0.31	3.6	12.9	0.95	1.0	5.1	1.00	21.7	34.7
2 (HA–NA)	8.8	0.96	6.8	0.95	-	-	-	2.4	9.0	0.97	0.9	6.2	1.00	16.3	160.3
3 (HD–NA)	6.9	0.94	5.7	0.94	-	-	-	5.2	15.7	0.98	0.6	3.7	0.95	12.5	70.5
4 (HA–HA or HD–HD)	7.5	0.97	7.2	0.97	-	-	-	4.0	11.1	1.00	5.6	9.6	1.00	13.5	104.4
5 (SA–NA)	40.0	0.83	14.9	0.93	5.2	24.0	0.96	9.0	44.1	0.88	4.9	13.8	0.37	32.4	200.0
6 (HD–HA)	6.0	0.93	6.1	0.93	-	-	-	3.5	21.5	1.00	2.0	9.6	1.00	23.6	43.1
7 (SA–HD)	15.2	0.85	12.3	0.85	-	-	-	-	-	-	2.4	9.6	0.85	84.4	188.0
8 (SA–HA)	24.9	0.92	15.7	0.90	24.5	17.4	1.00	12.9	28.4	0.84	3.9	11.0	0.64	37.2	164.4
9 (SA–SA)	33.9	0.89	22.6	0.89	4.2	13.3	1.00	5.6	13.2	0.96	6.6	24.4	0.45	39.6	182.4
overall	**16.6**	**0.93**	**11.3**	**0.93**	**8.9**	**19.5**	**0.82**	**5.5**	**18.1**	**0.94**	**6.6**	**9.2**	**0.74**	**30.5**	**139.6**

[a]The mixtures are classified in nine BACs, as proposed by Jaubert et al.[9] The abbreviations used for the associating character of a pure compound are as follows: NA for "nonassociating", HA for "hydrogen-acceptor", HD for "hydrogen-donor", and SA for "self-associating". Dots (-) indicate that no experimental data are available in the database for the respective properties.

- Case 2: $P_{ref} = 0$

As detailed in Appendix A1 of the Supporting Information, by combining eq 13 with eq 14 under zero pressure, we get

$$\frac{a_m}{b_m} = \sum_i z_i \frac{a_i}{b_i} + \frac{a_{res}^{E,\gamma}(T, \mathbf{z})}{\Lambda_{EoS}}$$
$$\text{with: } \Lambda_{EoS} = \frac{1}{r_2 - r_1} \ln\left(\frac{1 - r_2}{1 - r_1}\right) \tag{16}$$

Remarkably, the expressions of the MR for a_m/b_m obtained from the case at $P_{ref} = +\infty$ (eq 15) and $P_{ref} = 0$ (eq 16) are strictly identical. In consequence, the use of eq 13 to develop a MR for a_m/b_m seems particularly appropriate since the result is independent of the reference pressure (zero or infinite).

The proposed MR is summarized in eq 17

$$\begin{cases} b_m: \text{ any mixing rule} \\ \dfrac{a_m}{b_m} = \displaystyle\sum_i z_i \frac{a_i}{b_i} + \frac{a_{res}^{E,\gamma}}{\Lambda_{EoS}} \\ \text{with } \Lambda_{EoS} = \dfrac{1}{r_2 - r_1} \ln\left(\dfrac{1 - r_2}{1 - r_1}\right) \end{cases} \tag{17}$$

It is worth noting that the existing NRTL, WILSON, UNIQUAC, or UNIFAC parameters (e.g., compiled in the DECHEMA Chemistry Data Series) were determined at low pressure and low temperature [$P \leq \min(P_{c,i})$ and $T \leq \min(T_{c,i})$] and are supposed to be used with the γ–φ approach, assuming that the gas phase is ideal. On the contrary, the parameters to be used with the proposed MR were determined in larger domains of temperature and pressure that include the supercritical region in which the gas phase is far from being ideal. In addition, when the proposed MR is used, the combinatorial part of g^E stems from the EoS, and it is thus different from the one embedded in the NRTL, UNIQUAC, or WILSON ACM. For all these reasons, the existing parameters cannot be used with the proposed EoS/$a_{res}^{E,\gamma}$ MRs.

2.3. Implementation of the *tc*-PR-$a_{res}^{E,\gamma}$ Models. In this section, the *tc*-PR EoS (eq 1) coupled with EoS/$a_{res}^{E,\gamma}$ MRs (eq 17) that incorporate the residual part of the Wilson or UNIQUAC models or the $a_{res}^{E,\gamma}$ NRTL model is presented.

First of all, for the covolume of the mixture (b_m), the classical quadratic MR has been applied with the generalized formulation of the combining rule proposed by Lorentz for b_{ij}[23]

$$\begin{cases} b_m = \displaystyle\sum_i \sum_j z_i z_j b_{ij} \\ b_{ij} = \left(\dfrac{b_i^{1/s} + b_j^{1/s}}{2}\right)^s \end{cases} \tag{18}$$

where the parameter s has been set to 3/2. This specific value arises from optimization procedures aimed at selecting the s value, making it possible to reproduce the phase equilibria of athermal mixtures (typically mixtures containing two alkanes of different sizes) in an optimal way; for the sake of brevity, the detailed results—which are part of Le Guennec's thesis[24] —are detailed in Appendix A2 of the Supporting Information. Following Privat et al.'s advices,[3] a linear MR has been chosen

https://doi.org/10.1021/acs.iecr.1c03003
Ind. Eng. Chem. Res. 2021, 60, 17228–17247

Table 10. Rating of the Nine BACs in Order to Obtain the Final Mark of the PR−Van Laar Model[a]

BAC	mark on x	y	P_{LLV}	z_{LLV}	P_c	x_c	P_{az}	x_{az}	h^M	c_P^M	BAC mark	mark (over 20) by type of association	final mark of the PR−Van Laar model
1 (NA−NA)	15.6	15.4	6.0	3.2	16.5	12.9	19.5	17.5	14.6	16.5	13.8		
2 (HA−NA)	15.0	15.8	-	-	17.7	15.1	19.5	16.9	15.9	4.0	15.0	$\underbrace{\text{mark}_{NA}}_{\text{non-association}} = 14.9$	
3 (HD−NA)	15.6	16.2	-	-	15.8	11.9	18.8	17.3	16.9	13.0	15.7		
4 (HA−HA or HD−HD)	15.7	15.9	-	-	17.0	14.4	17.2	15.2	16.6	9.6	15.2		
5 (SA−NA)	**0.0**	11.6	16.7	7.7	11.7	**0.0**	6.5	4.9	11.9	**0.0**	7.1	$\underbrace{\text{mark}_{SA}}_{\text{self-association}} = 7.1$	**11.5/20**
6 (HD−HA)	15.8	15.7	-	-	17.4	9.2	19.0	15.2	14.1	15.7	15.3	$\underbrace{\text{mark}_{CA}}_{\text{cross-association}} = 15.3$	
7 (SA−HD)	10.5	11.7	-	-	-	-	15.9	12.9	**0.0**	1.2	8.7		
8 (SA−HA)	6.9	11.0	7.8	11.3	8.6	4.9	11.6	9.3	10.7	3.6	8.6	$\underbrace{\text{mark}_{CA+SA}}_{\text{cross-association +self-association}} = 8.9$	
9 (SA−SA)	2.7	7.7	17.9	13.3	15.2	12.9	8.8	3.5	10.1	1.8	9.4		
overall mark (eq 35)	**9.5**	**13.3**	**11.9**	**7.8**	**14.4**	**7.9**	**14.1**	**11.3**	**12.2**	**7.2**	**11.5**		

[a]Dots (-) indicate that no experimental data are available in the database for the respective properties.

for the volume-translation parameter: $c_m(\mathbf{z}) = \Sigma_i z_i \cdot c_i$. To sum up, when applied to a mixture, the *tc*-PR EoS takes the following expression

$$P(T, v, \mathbf{z}) = \frac{RT}{v + c_m - b_m} - \frac{a_m(T, \mathbf{z})}{(v + c_m)(v + c_m + b_m) + b_m(v + c_m - b_m)}$$

$$\text{with} \begin{cases} b_m = \sum_i \sum_j z_i z_j \left(\frac{b_i^{2/3} + b_i^{2/3}}{2} \right)^{3/2} \\ a_m = b_m \left[\sum_i z_i \frac{a_i}{b_i} + \frac{a_{res}^{E,\gamma}}{\Lambda_{PR}} \right] \\ \quad \text{with } \Lambda_{PR} = -\sqrt{2}/2 \cdot \ln(1 + \sqrt{2}) \\ c_m = \sum_i z_i \cdot c_i \end{cases} \tag{19}$$

2.3.1. tc-PR-Wilson Model. EoS/$a_{res}^{E,\gamma}$ MRs that combine the residual part of the Wilson[25] ACM (obtained by subtracting the combinatorial term from the complete model expression as follows: $a_{res}^{E,Wilson} = a^{E,Wilson} - a_{comb}^{E,Wilson}$) and the *tc*-PR EoS define the *tc*-PR-Wilson model hereafter.

For a binary system, the residual part of the $a^{E,Wilson}$ model is

$$\begin{cases} \frac{a_{res}^{E,Wilson}(T, \mathbf{z})}{RT} = \underbrace{\left\{ -z_1 \ln\left[z_1 + z_2 \frac{v_2^*}{v_1^*} \exp\left(-\frac{A_{12}}{T} \right) \right] - z_2 \ln\left[z_2 + z_1 \frac{v_1^*}{v_2^*} \exp\left(-\frac{A_{21}}{T} \right) \right] \right\}}_{a^{E,Wilson}/RT} \\ \quad - \underbrace{\left[z_1 \ln\left(\frac{v_1^*}{z_1 v_1^* + z_2 v_2^*} \right) + z_2 \ln\left(\frac{v_2^*}{z_1 v_1^* + z_2 v_2^*} \right) \right]}_{a_{comb}^{E,Wilson}/RT} \\ v_i^* \text{ was arbitrarily merged with the covolume (molar volume under infinite pressure) so that} \\ v_i^* = b_i - c_i \end{cases} \tag{20}$$

The two temperature-independent parameters A_{12} and A_{21} have to be fitted to experimental data.

It is worth recalling that the Wilson g^E/RT expression (first part of eq 20) is incapable of representing the liquid−liquid equilibria (LLE). This is because the instability criterion, that, for a binary system can be written: $\partial(x_i \cdot \gamma_i)/\partial x_i < 0$ is never violated.[26] In other words, whatever the values of the two parameters, the activity $(x_i \cdot \gamma_i)$ is always an increasing function of the composition (x_i). Tsuboka and Katayama[27] (TK) however demonstrated that the residual part of the Wilson model [eq 20], named the TK−Wilson model, was able to reproduce the LLE. In short, such a deficiency of the Wilson model is due to the simultaneous presence of the combinatorial (of Flory type) and residual parts of the Wilson model. By removing the combinatorial part, the Wilson ACM recovers its capacity to predict LLE. The results obtained in this paper (see the following sections) highlight that the combination of the residual part of the Wilson model and a CEoS in which the combinatorial part of g^E is given by eq 11 totally fixes this deficiency. The *tc*-PR-Wilson model was indeed able to accurately correlate the LLE and vapor−liquid−liquid equilibrium (VLLE) data that are included in the reference database developed by Jaubert el al.[9]

2.3.2. tc-PR-UNIQUAC Model. EoS/$a_{res}^{E,\gamma}$ MRs that combine the residual part of the UNIQUAC[28] ACM ($a_{res}^{E,UNIQUAC}$) and the *tc*-PR EoS define the *tc*-PR-UNIQUAC model hereafter. For a binary system, the residual part of the $a^{E,UNIQUAC}$ model is

$$\frac{a_{res}^{E,UNIQUAC}(T, \mathbf{z})}{RT} = -q_1 z_1 \ln\left[\frac{z_1 q_1}{z_1 q_1 + z_2 q_2} + \frac{z_2 q_2}{z_1 q_1 + z_2 q_2} \exp\left(-\frac{A_{12}}{T} \right) \right] - q_2 z_2 \ln\left[\frac{z_2 q_2}{z_1 q_1 + z_2 q_2} + \frac{z_1 q_1}{z_1 q_1 + z_2 q_2} \exp\left(-\frac{A_{21}}{T} \right) \right] \tag{21}$$

q_1 and q_2 are the van der Waals surface areas of molecules 1 and 2 divided by a reference surface of $2.5 \times 10^9 \text{cm}^2 \cdot \text{mol}^{-1}$ in order to obtain dimensionless parameters. In this paper, they were extracted from the DIPPR database. Temperature-independent parameters A_{12} and A_{21} have to be fitted to the experimental data.

2.3.3. tc-PR-NRTL Model. EoS/$a_{res}^{E,\gamma}$ MRs that combine the purely residual NRTL[29] ACM ($a_{res}^{E,NRTL} = a^{E,NRTL}$) and the *tc*-PR EoS define the *tc*-PR-NRTL model hereafter. For a binary system, the NRTL model is

https://doi.org/10.1021/acs.iecr.1c03003
Ind. Eng. Chem. Res. 2021, 60, 17228−17247

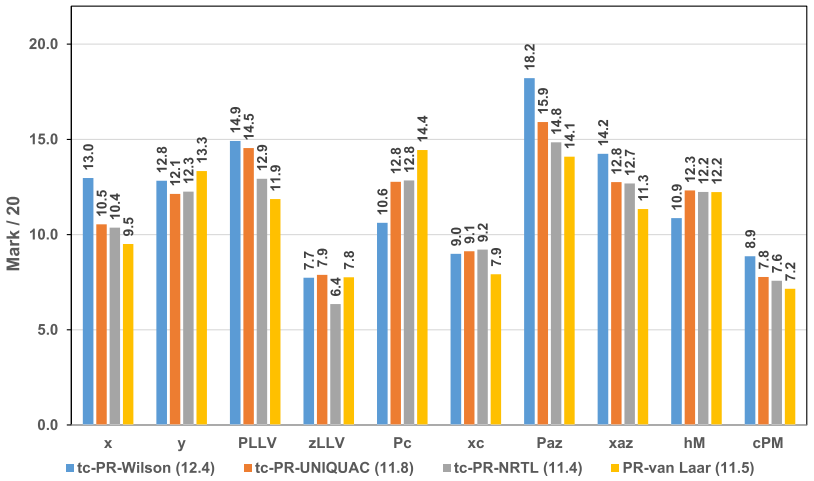

Figure 2. Overview of the accuracy of the *tc*-PR-Wilson, *tc*-PR-UNIQUAC, *tc*-PR-NRTL, and PR−Van Laar models by plotting the overall marks per property (prop ∈ {x, y, P_{LLV}, z_{LLV}, P_c, x_c, P_{azeo}, x_{azeo}, h^M, c_P^M}), as calculated by eq 35. The complete database, that is the 200 binary systems are considered here.

$$\frac{a_{res}^{E,NRTL}(T,\mathbf{z})}{RT} = z_1 z_2 \left[\frac{\frac{A_{21}}{T}\exp\left(-\alpha\frac{A_{21}}{T}\right)}{z_1 + z_2\exp\left(-\alpha\frac{A_{21}}{T}\right)} + \frac{\frac{A_{12}}{T}\exp\left(-\alpha\frac{A_{12}}{T}\right)}{z_2 + z_1\exp\left(-\alpha\frac{A_{12}}{T}\right)} \right] \tag{22}$$

The parameter α has been set to 0.3, and the two temperature-independent ones (A_{12} and A_{21}) were fitted to the experimental data.

2.4. Implementation of the PR−Van Laar Model. It is worth recalling that the first benchmarked model against the binary system database proposed by Jaubert et al.[9] was the PR EoS armed with classical van der Waals mixing and combining rules (eqs 5−8) with $l_{12} = l_{21} = 0$ and temperature-dependent BIPs ($k_{12}(T) = k_{21}(T)$) calculated as

$$k_{12}(T) = \frac{A_{12}\cdot\left(\frac{298.15}{T}\right)^{(B_{12}/A_{12}-1)} - \left(\frac{\sqrt{a_1(T)}}{b_1} - \frac{\sqrt{a_2(T)}}{b_2}\right)^2}{2\frac{\sqrt{a_1(T)\cdot a_2(T)}}{b_1\cdot b_2}} \tag{23}$$

Temperature-independent parameters $A_{12} = A_{21}$ and $B_{12} = B_{21}$ were fitted over the available experimental data.

Such a model can also be seen[30,31] as the PR EoS coupled with EoS/$a_{res}^{E,\gamma}$ MRs involving the purely residual Van Laar $a^{E,\gamma}$ model. For a binary system, the Van Laar model reads

$$\begin{cases} \dfrac{a_{res}^{E,VanLaar}(T,\mathbf{z})}{RT} = \dfrac{-\Lambda_{PR}}{RT}\cdot\dfrac{z_1 z_2 b_1 b_2 E_{12}(T)}{z_1 b_1 + z_2 b_2} \\ \text{The unique } E_{12} \text{ parameter varies with } T \text{ according to:} \\ E_{12}(T) = A_{12}\cdot\left(\dfrac{298.15}{T}\right)^{(B_{12}/A_{12}-1)} \end{cases} \tag{24}$$

Equation 24 shows that the Van Laar model is in fact a one-parameter $a^{E,\gamma}$ model (E_{12}). Such a unique parameter is however temperature-dependent so that at the end, two parameters per binary system (A_{12} and B_{12}) have to be fitted on the experimental data.

Similar to the *tc*-PR-Wilson, *tc*-PR-UNIQUAC, and *tc*-PR-NRTL model, the PR−Van Laar model is an extension of the PR EoS to mixtures with the help of advanced EoS/$a_{res}^{E,\gamma}$ MRs.

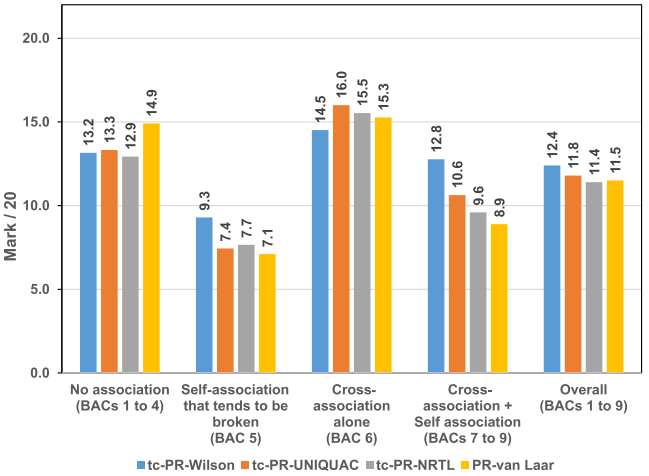

Figure 3. Overview of the accuracy of the *tc*-PR-Wilson, *tc*-PR-UNIQUAC, *tc*-PR-NRTL, and PR−Van Laar models by plotting the average marks for the four categories of binary systems based on the type of association they exhibit (refer to Table S1 in Appendix A3 of the Supporting Information).

However, contrary to the *tc*-PR-Wilson, *tc*-PR-UNIQUAC, and *tc*-PR-NRTL models, the PR−Van Laar model is not translated and includes in its formulation a linear MR for the covolume and a nonconsistent Soave α-function. It thus cannot be named *tc*-PR-Van Laar. In other words, it cannot be considered as an extension of the *tc*-PR EoS to mixtures. On the other hand, similarly to the *tc*-PR-$a_{res}^{E,\gamma}$ models, the PR−Van Laar model contains two adjustable parameters. Since it was the first model to be graded against the database proposed by Jaubert et al.,[9] we found it pertinent to include the PR−Van Laar model in the comparison and grading of the three *tc*-PR-$a_{res}^{E,\gamma}$ models selected in this study. Our plan is to use the PR−Van Laar model as a reference model for discussing the capabilities and weaknesses of the studied *tc*-PR-$a_{res}^{E,\gamma}$ models.

Note that as mentioned before, two temperature-independent adjustable parameters per model were fitted to the experimental data. For this purpose, it was decided to select the same objective function as Jaubert et al.[9] The regressed BIPs for the three *tc*-PR-$a_{res}^{E,\gamma}$ and the PR−Van Laar models are reported in Appendix A3 of the Supporting Information.

https://doi.org/10.1021/acs.iecr.1c03003
Ind. Eng. Chem. Res. 2021, 60, 17228−17247

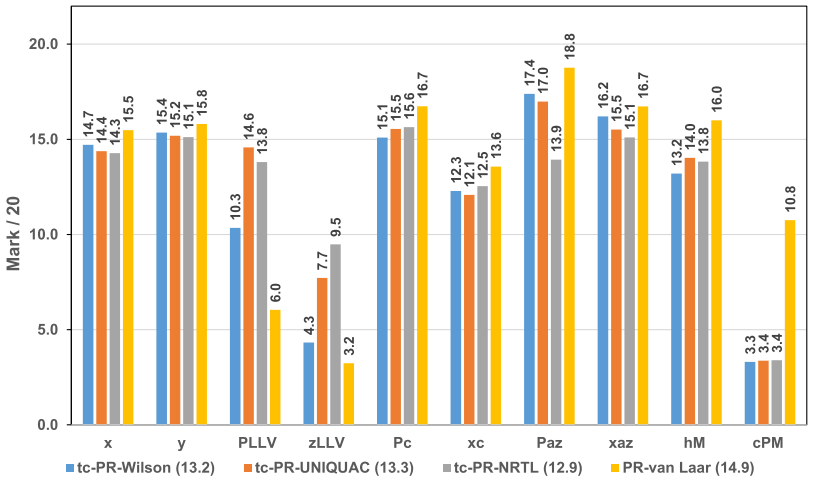

Figure 4. Overview of the accuracy of the *tc*-PR-Wilson, *tc*-PR-UNIQUAC, *tc*-PR-NRTL, and PR−Van Laar models by plotting the marks on 10 properties for the category including mixtures without association (BACs 1−4).

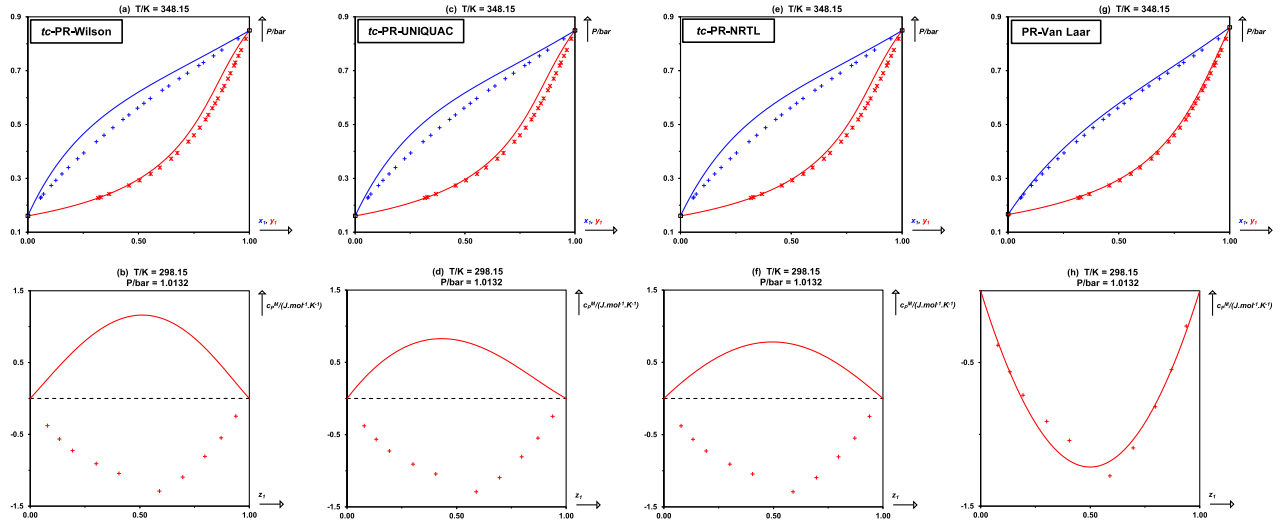

Figure 5. Pressure−composition VLE phase diagrams (top) and mixing heat capacity−composition diagrams (bottom) for the binary system cyclohexane (1) + monochlorobenzene calculated with the *tc*-PR-Wilson (a,b), *tc*-PR-UNIQUAC (c,d), *tc*-PR-NRTL (e,f), and PR−Van Laar (g,h) models. Phase equilibrium diagram convention: (red *): experimental dew points; (blue +): experimental bubble points; (red −): calculated dew curve; and (blue −): calculated bubble curve. Caloric property diagram convention: (red +): experimental data and (red −): calculated curve.

It also should be noted that using temperature-independent parameters for the three *tc*-PR-$a_{res}^{E,\gamma}$ models is the first step before moving to more complex and more accurate approaches. Indeed, from our experience, ignoring the temperature dependency of the two parameters embedded in the activity-coefficient models typically leads to less accurate results.

3. GRADING OF THE *tc*-PR-WILSON, *tc*-PR-UNIQUAC, AND *tc*-PR-NRTL MODELS

In this section, the performances of three *tc*-PR-$a_{res}^{E,\gamma}$ and PR−Van Laar models are presented. First, the grading procedure proposed by Jaubert et al.[9] is briefly summarized. Then, some modifications on the grading are presented in order to better consider the impact of the *out-of-model* points in the final mark. This is indeed an issue that emerged as important during the grading of the PC-SAFT EoS with zero k_{ij}.[10] Finally, the results of the grading procedure are discussed.

3.1. Grading Procedure. A methodology was developed recently by Jaubert and co-workers toward addressing the issue of model reliability and grading.[9] A high-quality reference database was built that can be used for assessing the accuracy of a thermodynamic model or to cross-compare the performances of different models.[9] A specific procedure for the calculation of the deviations between model calculations and experimental data was discussed in detail, and a methodology for grading a thermodynamic model was proposed. In total, 200 nonelectrolytic binary mixtures were selected to cover all categories of mixtures. They were divided into nine groups (each characterized by a so-called binary association code, BAC) according to the associating character of the two components, that is, to their ability to be involved in a hydrogen bond (see Table S1 in Appendix A3 of the Supporting Information). During the grading of a thermodynamic model, only four categories of binary systems are retained based on the type of association they exhibit (see the last column of Table S1 in Appendix A3 of the Supporting Information).

In general, for each binary system of the database, 10 properties were experimentally determined: liquid-phase

https://doi.org/10.1021/acs.iecr.1c03003
Ind. Eng. Chem. Res. 2021, 60, 17228−17247

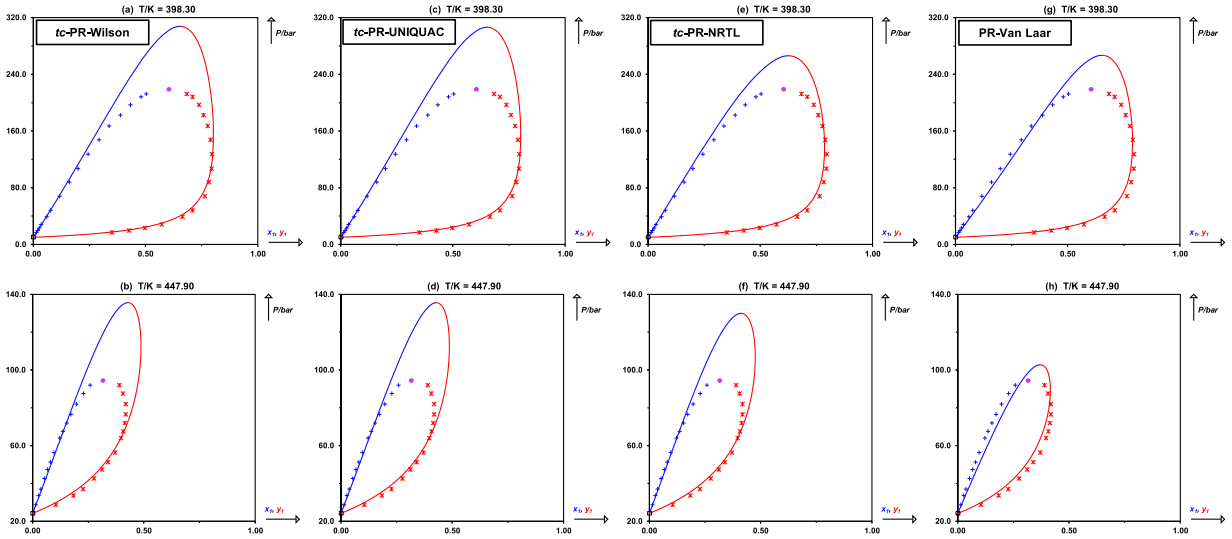

Figure 6. Pressure−composition VLE phase diagrams for the binary system N_2 (1) + *n*-pentane calculated with the *tc*-PR-Wilson (a,b), *tc*-PR-UNIQUAC (c,d), *tc*-PR-NRTL (e,f), and PR−Van Laar (g,h) models. Phase equilibrium diagram convention: (red *): experimental dew points; (blue +): experimental bubble points; (violet ○): experimental critical point; (red −): calculated dew curve; and (blue −): calculated bubble curve.

composition x, gas-phase composition (or second liquid-phase composition) y, three-phase pressure P_{LLV}, three-phase composition z_{LLV}, critical pressure P_c, critical composition x_c, azeotropic pressure P_{azeo}, azeotropic composition x_{azeo}, mixing enthalpy h^M, and mixing heat capacity c_P^M.

The grading procedure proposed by Jaubert et al.[9] consists of the following main steps

1. For each of the nine BACs, the mean average percentage error (MAPE) between model calculations and experimental data for each type of available experimental properties (10 at the most) is calculated as follows

$$\mathrm{MAPE}_{\mathrm{prop}}^{\mathrm{BAC}_i}(\%) = \frac{1}{N_{\mathrm{data}}}\sum_{j=1}^{N_{\mathrm{data}}} 100\cdot \left|\frac{\mathrm{PROP}_j^{\mathrm{EXP}} - \mathrm{PROP}_j^{\mathrm{MODEL}}}{\mathrm{PROP}_j^{\mathrm{EXP}}}\right| \tag{25}$$

2. For a given BAC, a mark (max score is 20) is then calculated for each type of available experimental properties. At the end, a BAC receives 10 marks at the most depending on the availability of the experimental data. For an available experimental property (denoted prop), prop ∈ {x, y, P_{LLV}, z_{LLV}, P_c, x_c, P_{azeo}, x_{azeo}, h^M, c_P^M}, the general mark expression is given by

$$\mathrm{Mark}_{\mathrm{prop}}^{\mathrm{BAC}_i} = 20 - \alpha_{\mathrm{prop}}\cdot \mathrm{MAPE}_{\mathrm{prop}}^{\mathrm{BAC}_i} \tag{26}$$

where $\alpha_{\mathrm{prop}} = 0.5$ with the exception of $\alpha_{P_c} = 0.75$, $\alpha_h^M = 0.25$, and $\alpha_{c_P^M} = 0.10$. Any mark below zero is increased to zero. For important details and the exact methodology, the reader is referred to the original publication.[9]

3. The mark attributed to a given BAC is calculated by averaging the marks received by the available experimental properties of such a BAC (given at step 2)

$$\mathrm{mark}^{\mathrm{BAC}_i} = \mathrm{avg}\left(\begin{array}{ccccc} \mathrm{mark}_{x_{\mathrm{or}}x_\alpha}^{\mathrm{BAC}_i}; & \mathrm{mark}_{y_{\mathrm{or}}x_\beta}^{\mathrm{BAC}_i}; & \mathrm{mark}_{P_{\mathrm{LLV}}}^{\mathrm{BAC}_i}; & \mathrm{mark}_{z_{\mathrm{LLV}}}^{\mathrm{BAC}_i}; & \mathrm{mark}_{P_c}^{\mathrm{BAC}_i}; \\ \mathrm{mark}_{x_c}^{\mathrm{BAC}_i}; & \mathrm{mark}_{P_{\mathrm{az}}}^{\mathrm{BAC}_i}; & \mathrm{mark}_{x_{\mathrm{az}}}^{\mathrm{BAC}_i}; & \mathrm{mark}_{h^M}^{\mathrm{BAC}_i}; & \mathrm{mark}_{c_P^M}^{\mathrm{BAC}_i} \end{array}\right) \tag{27}$$

4. Calculation of the marks for the four categories of binary systems retained according to the type of association they exhibit (see the last column of Table S1 in Appendix A3 of the Supporting Information) by averaging the marks of the BACs belonging to each of them.

$$\begin{cases} \mathrm{mark}_{\substack{\text{mixtures without}\\ \text{association}}} = \dfrac{\mathrm{mark}^{\mathrm{BAC}_1} + \mathrm{mark}^{\mathrm{BAC}_2} + \mathrm{mark}^{\mathrm{BAC}_3} + \mathrm{mark}^{\mathrm{BAC}_4}}{4} \\ \mathrm{mark}_{\substack{\text{mixtures with}\\ \text{self-association}}} = \mathrm{mark}^{\mathrm{BAC}_5} \\ \mathrm{mark}_{\substack{\text{mixtures with}\\ \text{cross-association}}} = \mathrm{mark}^{\mathrm{BAC}_6} \\ \mathrm{mark}_{\substack{\text{mixtures with}\\ \text{cross-association}\\ \text{and self-association}}} = \dfrac{\mathrm{mark}^{\mathrm{BAC}_7} + \mathrm{mark}^{\mathrm{BAC}_8} + \mathrm{mark}^{\mathrm{BAC}_9}}{3} \end{cases} \tag{28}$$

5. Calculation of the final mark of the thermodynamic model by averaging the mark of the four considered categories of binary systems (determined at step 4).

$$\underset{\substack{\text{of a thermodynamic}\\ \text{model (over20)}}}{\text{Final mark}} = \frac{1}{4}\times \underbrace{\left[\mathrm{mark}_{\substack{\text{mixtures without}\\ \text{association}}} + \mathrm{mark}_{\substack{\text{mixtures with}\\ \text{self-association}}} + \mathrm{mark}_{\substack{\text{mixtures with}\\ \text{cross-association}}} + \mathrm{mark}_{\substack{\text{mixtures with}\\ \text{cross-association}\\ \text{and self-association}}}\right]}_{\text{average of 4 marks}} \tag{29}$$

In this work, two modifications to the original grading procedure are introduced. The first one tends to correct the difference of treatment in the calculation of the deviation on the fluid-phase compositions depending on whether they belong or not to a three-phase line. Indeed, as pointed out by Jaubert et al.,[9] very small mole fractions (or very close to 1) may lead to huge percentage deviations and introduce a bias in the $\mathrm{mark}_{z_{\mathrm{LLV}}}^{\mathrm{BAC}_i}$ attributed to a given BAC. To avoid this issue, it is necessary to determine for each three-phase line of a given BAC (one after the other) the absolute relative deviation ($\mathrm{ARD}_{z_{\mathrm{LLV}}}^{3-\varphi\mathrm{line}}$) between the calculated and experimental compositions by

https://doi.org/10.1021/acs.iecr.1c03003
Ind. Eng. Chem. Res. 2021, 60, 17228−17247

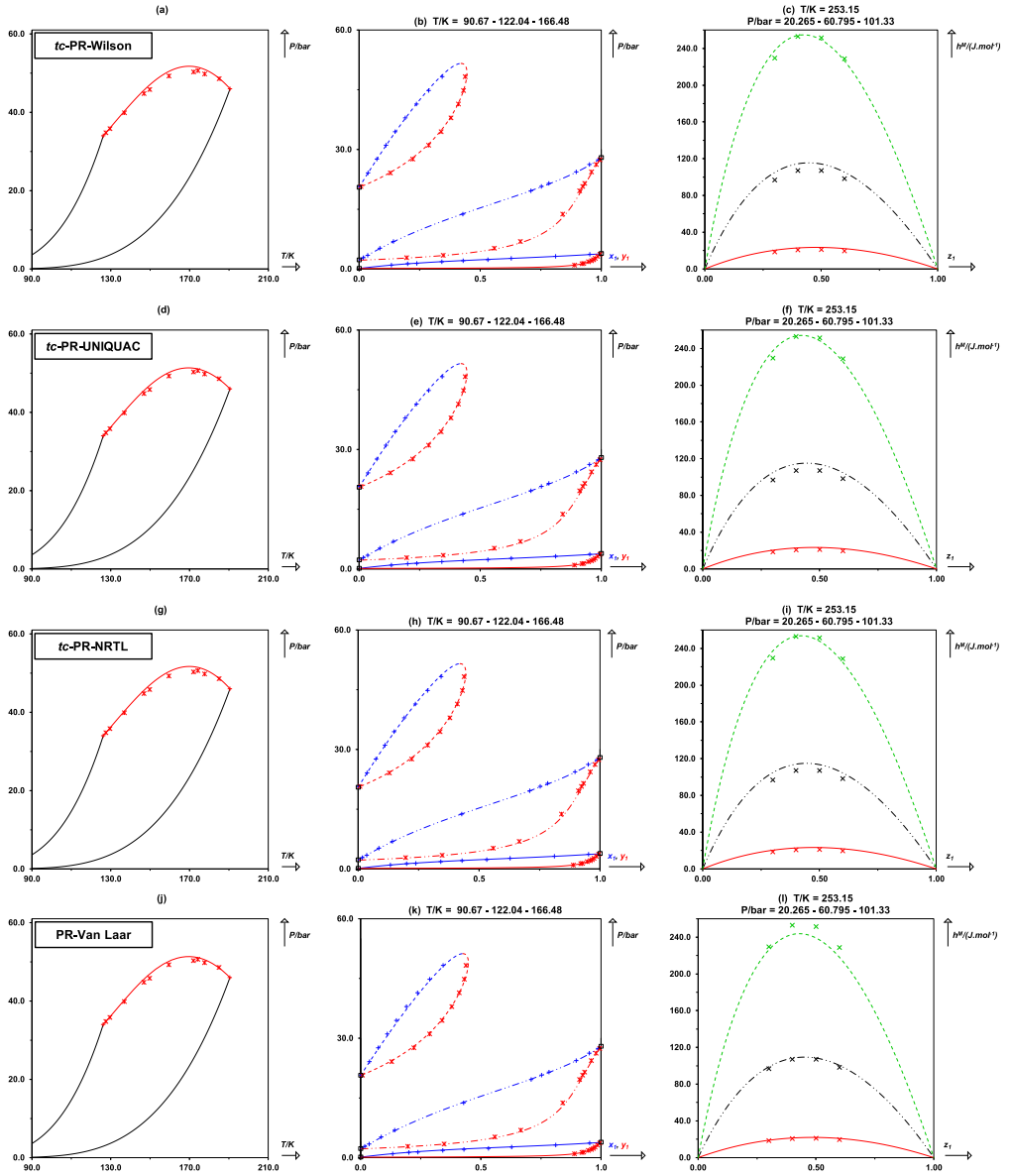

Figure 7. Global phase equilibrium diagrams (GPEDs) (left), pressure−composition VLE phase diagrams (center), and mixing heat capacity−composition diagrams (right) for the binary system N_2 (1) + methane calculated with the *tc*-PR-Wilson (a−c), *tc*-PR-UNIQUAC (d−f), *tc*-PR-NRTL (g−i), and PR−Van Laar (j−l) models. GPED convention: (red *) experimental critical points; (red −) calculated critical line; and (black −): calculated vapor−pressure curves of pure components. Phase equilibrium diagram convention: (red *): experimental dew points; (blue +): experimental bubble points; (red −): calculated dew curve; and (blue −): calculated bubble curve.

$$\begin{cases} \mathrm{ARD}_{z_{\mathrm{LLV}}}^{3-\varphi\mathrm{line}} = \\ \quad \sum_{j=1}^{2}\left[\dfrac{\text{ARD on } x_j^{\alpha}(\%) + \text{ARD on } x_j^{\beta}(\%) + \text{ARD on } y_j(\%)}{6}\right] \end{cases} \tag{30}$$

$$\text{with: ARD on } z_j(\%) = 100\cdot\left|\frac{z_j^{\mathrm{EXP}} - z_j^{\mathrm{MODEL}}}{z_j^{\mathrm{EXP}}}\right| \tag{31}$$

where x_j^{α}, x_j^{β}, and y_j are the mole fractions of component j in each of the three equilibrium phases.

In this work, it was decided to apply the same procedure to eq 30 as the one used to calculate the deviations on the liquid- or gas-phase composition of a classical VLE data point. Consequently, if z_1 stands for the mole fraction of component 1 in one of the three phases ($z_1 = x_1^{\alpha}$, x_1^{β}, and/or y_1), an experimental phase composition is *rejected* (and thus is not taken into account in eq 30 in order to annihilate its influence on the calculated $\mathrm{ARD}_{z_{\mathrm{LLV}}}^{3-\varphi\mathrm{line}}$), provided

$$\begin{cases} z_{1,\mathrm{exp}} < 0.01 \text{ or } z_{1,\mathrm{exp}} > 0.99 \\ \text{and simultaneously } 1/2 \times (\text{ARD on } z_1 + \text{ARD on } z_2) > 45\% \end{cases} \tag{32}$$

This modification makes it compulsory in eq 30 to keep only the deviations on the three-phase line compositions passing the test introduced in eq 32. Indeed, for a given three-phase line, the calculation of $\mathrm{ARD}_{z_{\mathrm{LLV}}}^{3-\varphi\mathrm{line}}$ depends on how many phases, and their respective mole fractions, are rejected. As an example, in the case where only one phase composition out of the three is rejected, four deviations (instead of six) are calculated, and the denominator of eq 30 must be adapted accordingly. Similarly, if two phase compositions among the three are

https://doi.org/10.1021/acs.iecr.1c03003
Ind. Eng. Chem. Res. 2021, 60, 17228−17247

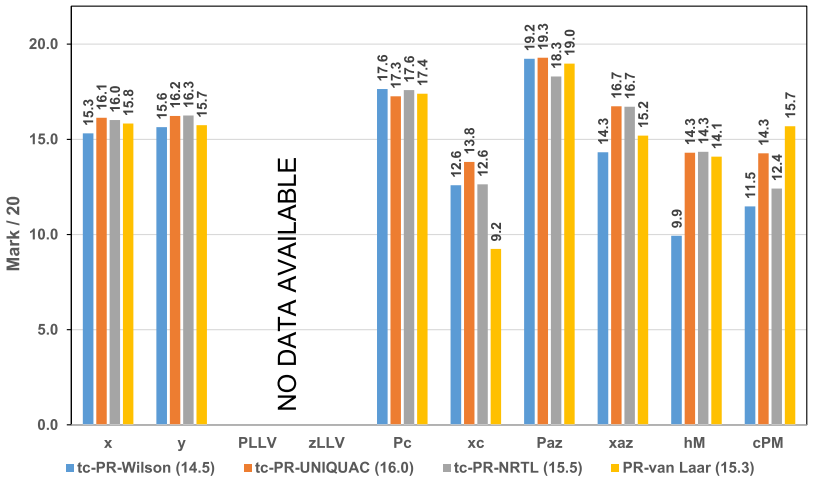

Figure 8. Overview of the accuracy of the *tc*-PR-Wilson, *tc*-PR-UNIQUAC, *tc*-PR-NRTL, and PR−Van Laar models by plotting the marks on 10 properties for the category including mixtures in which cross-association alone takes place (BAC 6).

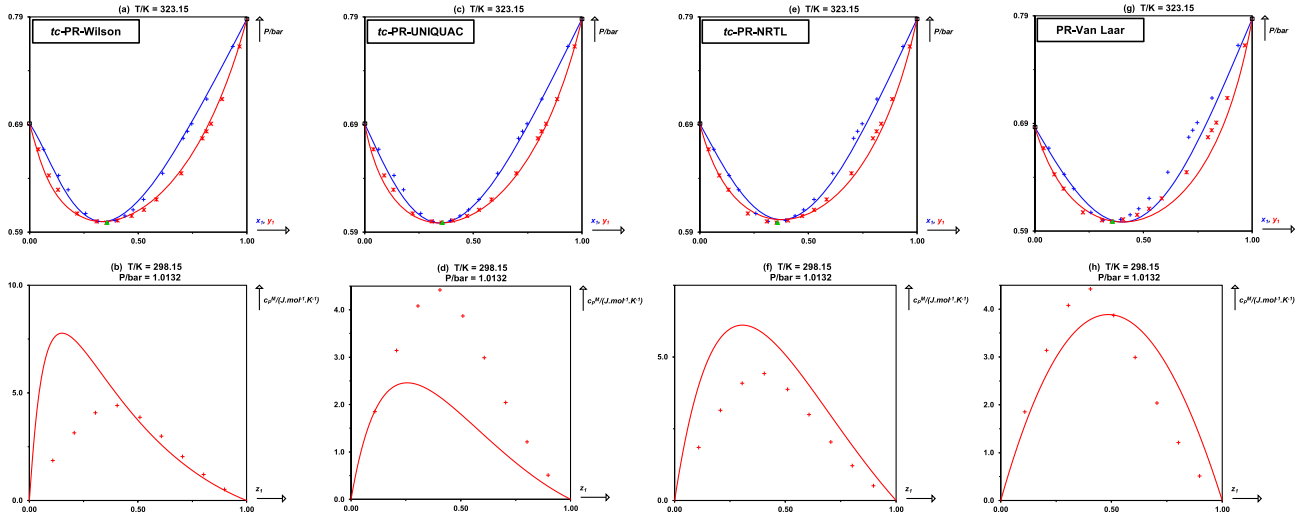

Figure 9. Pressure−composition VLE phase diagrams (top) and mixing heat capacity−composition diagrams (bottom) for the binary system methyl acetate (1) + chloroform calculated with the *tc*-PR-Wilson (a,b), *tc*-PR-UNIQUAC (c,d), *tc*-PR-NRTL (e,f), and PR−Van Laar (g,h) models. Phase equilibrium diagram convention: (red *): experimental dew points; (blue +): experimental bubble points; (green ▲): experimental azeotropic point; (red −): calculated dew curve and; (blue −): calculated bubble curve. Caloric property diagram convention: (red +): experimental data and; (red −): calculated curve.

rejected, only two deviations will be calculated and included in eq 30. Finally, if the compositions of the three phases are rejected, no $\mathrm{ARD}_{z_{\mathrm{LLV}}}^{3-\varphi\mathrm{line}}$ is calculated for such a three-phase line. In this latter case, we apply $N_{3-\varphi\mathrm{lines}}^{\mathrm{BAC}_i} = N_{3-\varphi\mathrm{lines}}^{\mathrm{BAC}_i} - 1$, where $N_{3-\varphi\mathrm{lines}}^{\mathrm{BAC}_i}$ designates the number of three-phase lines for which an ARD could be calculated.

Once done, for a given BAC, the calculation of the mark on z_{LLV} is straightforward

$$\mathrm{mark}_{z_{\mathrm{LLV}}}^{\mathrm{BAC}_i} = 20 - 0.5 \times \frac{1}{N_{3-\varphi\mathrm{lines}}^{\mathrm{BAC}_i}} \sum_{j=1}^{N_{3-\varphi\mathrm{lines}}^{\mathrm{BAC}_i}} \mathrm{ARD}_{z_{\mathrm{LLV}}}^{3-\varphi\mathrm{line}} \tag{33}$$

The second modification is related to the inclusion of the *out-of-model* (OM) points in the grading procedure. Before discussing the details of such a modification, it would be pertinent to recall the definition of an *out-of-model* point. An experimental point is considered *out-of-model* if the thermodynamic model does not predict its existence, and in consequence, the experimental value cannot be compared to a calculated one and thus cannot be considered in a MAPE calculation. For instance, it may happen that a model does not predict the existence of a homogeneous azeotrope that is experimentally observed, however. For a more detailed explanation, the reader is referred to Jaubert et al.[9]

For the purpose of this section, that is, to better understand the influence of OM data points, consider the case presented in Figure 1. Recalling that deviations over bubble and dew-point compositions are calculated at the temperature and pressure of the experimental data, one observes that there are more *out-of-model* points in Figure 1b than in Figure 1a. In consequence, the number of data points considered in the MAPE calculation is greater in case A than that in case B. It may happen that the consideration of more points in the MAPE calculation (case A) results in a higher MAPE value than that in the case where less data points are taken into account (case B). In the illustration example considered here, the MAPE for case B appears lower, while the calculated phase-diagram does not have the right

https://doi.org/10.1021/acs.iecr.1c03003
Ind. Eng. Chem. Res. 2021, 60, 17228−17247

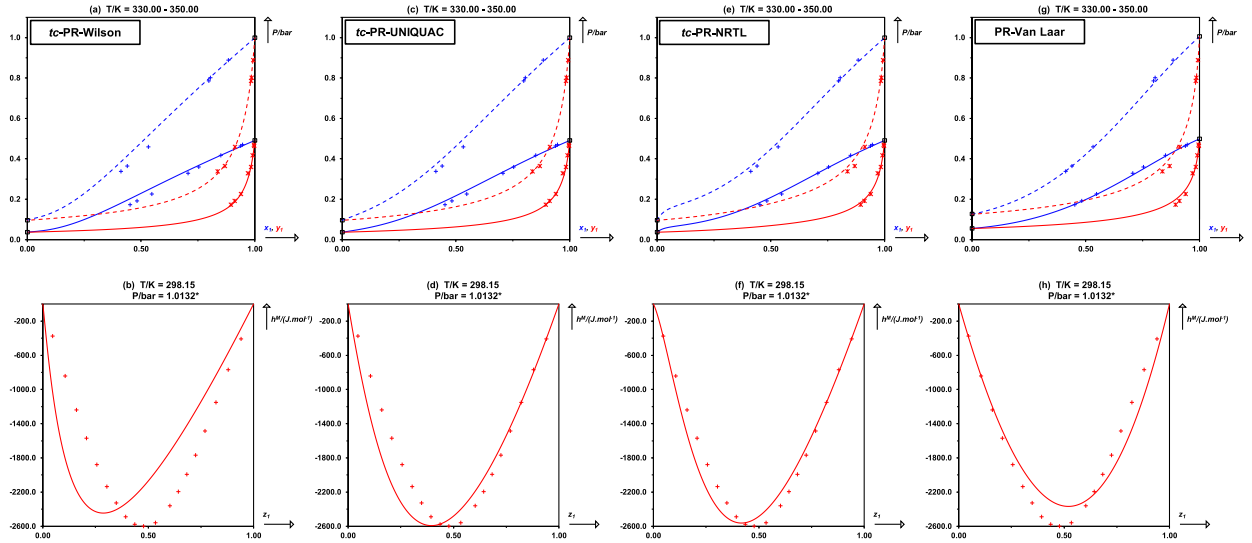

Figure 10. Pressure−composition VLE phase diagrams (top) and mixing heat capacity−composition diagrams (bottom) for the binary system ethyl acetate (1) + 1,1,2,2-tetrachloroethane calculated with the *tc*-PR-Wilson (a,b), *tc*-PR-UNIQUAC (c,d), *tc*-PR-NRTL (e,f), and PR−Van Laar (g,h) models. Phase equilibrium diagram convention: (red *): experimental dew points; (blue +): experimental bubble points; (red −): calculated dew curve and; (blue −): calculated bubble curve. Caloric property diagram convention: (red +): experimental data and; (red −): calculated curve.

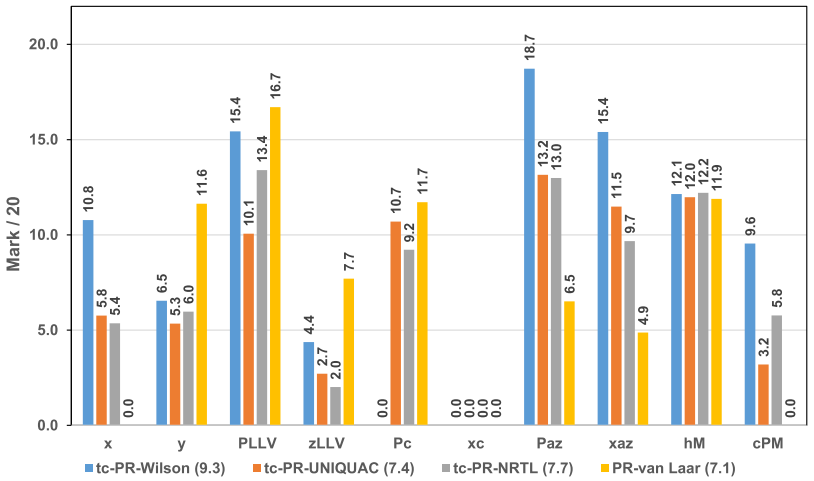

Figure 11. Overview of the accuracy of the *tc*-PR-Wilson, *tc*-PR-UNIQUAC, *tc*-PR-NRTL, and PR−Van Laar models by plotting the marks on 10 properties for the category including mixtures in which self-association tends to be broken (BAC 5).

magnitude. To illustrate this and for the sake of simplicity, consider only the MAPE on x. For case A in Figure 1, MAPE_x^{A} = 10.6% is obtained over nine points, while for case B, four points are declared *out-of-model*, which results in MAPE_x^{B} = 7.7% over five points. The marks for case A and B are 14/20 and 16/20, respectively. It does not seem fair at all since graphically, the model associated with case A has a better predictive capacity than the model associated with case B since it can predict the existence of more data points.

In order to avoid this type of issue, a slight modification in the second step of the grading procedure is introduced. For a given BAC_i, the calculation of the mark for property *prop* becomes

$$\begin{cases} \text{mark}_{\text{prop}}^{\text{BAC}_i} = (20 - \alpha_{\text{prop}} \cdot \text{MAPE}_{\text{prop}}^{\text{BAC}_i}) \cdot \underbrace{\text{SR}_{\text{prop}}^{\text{BAC}_i}}_{\text{success ratio}} \\ \text{SR}_{\text{prop}}^{\text{BAC}_i} = 1 - \dfrac{N_{\text{OM,prop}}^{\text{BAC}_i}}{N_{\text{exp ,prop}}^{\text{BAC}_i}} \\ \text{prop} \in \{x,\ y,\ P_{\text{LLV}},\ z_{\text{LLV}},\ P_{\text{c}},\ x_{\text{c}},\ P_{\text{azeo}},\ x_{\text{azeo}},\ h^{\text{M}},\ c_{\text{P}}^{\text{M}}\} \end{cases} \tag{34}$$

$\text{SR}_{\text{prop}}^{\text{BAC}_i}$ corresponds to the "success ratio" of the model to reproduce property *prop* for binary systems involved in BAC_i. $N_{\text{OM,prop}}^{\text{BAC}_i}$ and $N_{\text{exp ,prop}}^{\text{BAC}_i}$ are the number of *out-of-model* points and the number of experimental data points for property *prop* for binary systems available in BAC_i, respectively. Therefore, $\text{SR}_{\text{prop}}^{\text{BAC}_i}$ represents the actual fraction of the number of points not declared *out-of-model* (i.e., the number of points for which a deviation between the calculated and experimental data can be evaluated divided by the number of experimental points).

https://doi.org/10.1021/acs.iecr.1c03003
Ind. Eng. Chem. Res. 2021, 60, 17228−17247

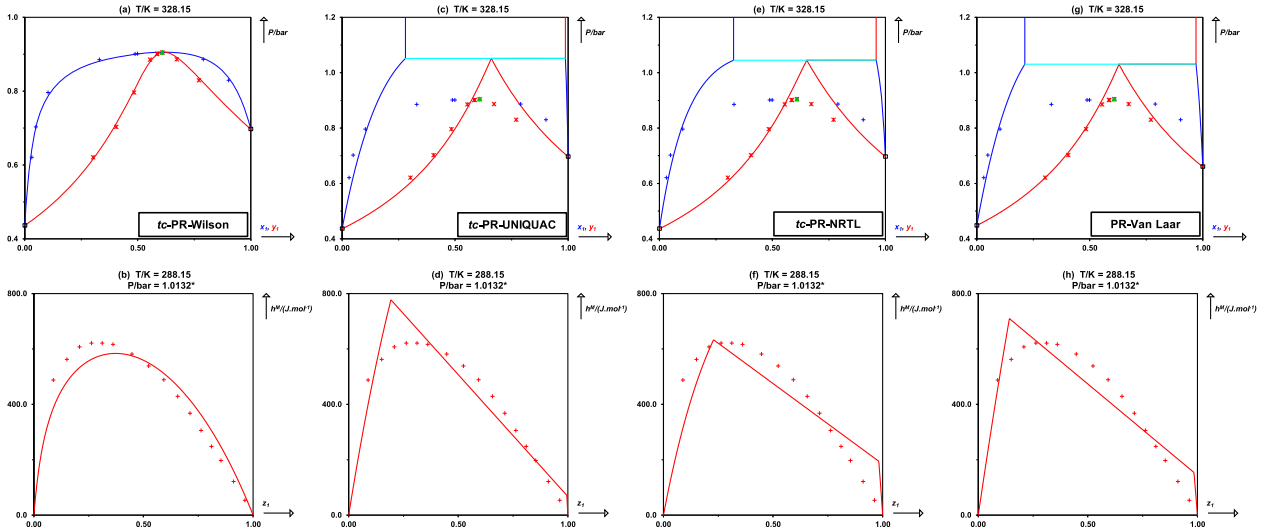

Figure 12. Pressure−composition VLE phase diagrams (top) and mixing enthalpy−composition diagrams (bottom) for the binary system methanol (1) + benzene calculated with the *tc*-PR-Wilson (a,b), *tc*-PR-UNIQUAC (c,d), *tc*-PR-NRTL (e,f), and PR−Van Laar (g,h) models. Phase equilibrium diagram convention: (red *): experimental dew points; (blue +): experimental bubble points; (green ▲): experimental azeotropic point; (red −): calculated dew curve; (blue −): calculated bubble curve and; (teal −): calculated three-phase line. Caloric property diagram convention: (red +): experimental data and; (red −): calculated curve.

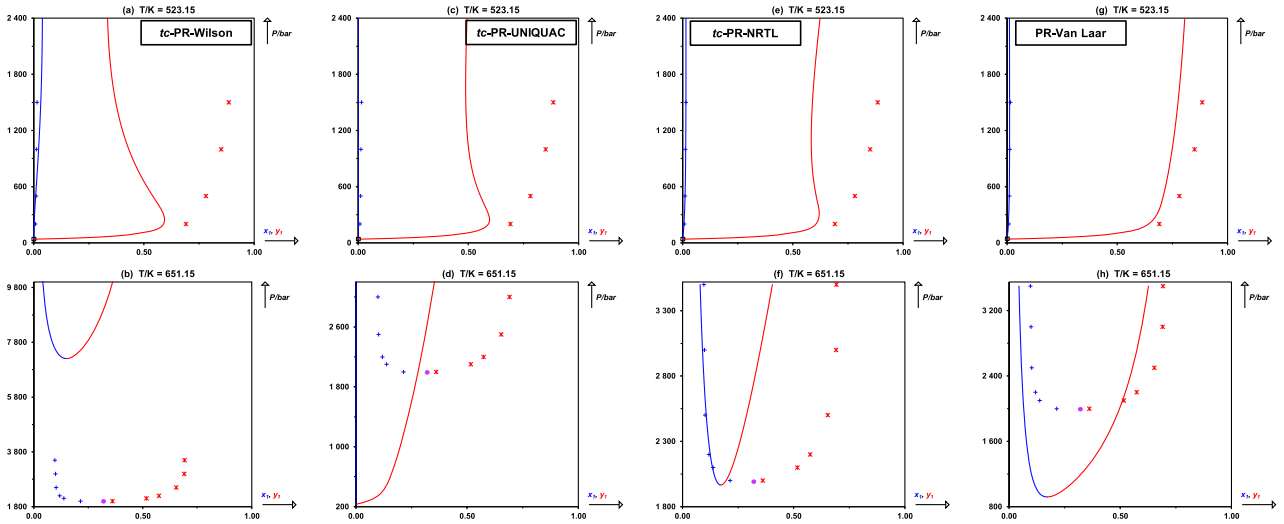

Figure 13. Pressure−composition VLE phase diagrams for the binary system ethane (1) + water calculated with the *tc*-PR-Wilson (a,b), *tc*-PR-UNIQUAC (c,d), *tc*-PR-NRTL (e,f), and PR−Van Laar (g,h) models. Phase equilibrium diagram convention: (red *): experimental dew points; (blue +): experimental bubble points; (violet ○): experimental critical point; (red −): calculated dew curve and; (blue −): calculated bubble curve.

For clarity, let us here recall that *out-of-model* data points do not occur for enthalpy and heat capacity of mixing data because it is always possible to calculate these properties at specified T, P, and z_1 values. It follows that the success ratio is always equal to 1 for h^M and c_P^M.

Coming back to the example of Figure 1, for case A, $MAPE_x^A$ = 10.6% and SR_x^A = 1 (100% of the experimental data were predicted by the model), and for case B, $MAPE_x^B$ = 7.7% and SR_x^B = 5/9 = 0.56 (only 56% of the experimental data were predicted by the model). It results in marks (over 20) of 14 and 9 for cases A and B, respectively. Such a result agrees with what is expected from a model evaluation procedure.

We can here assert that this second modification of the grading procedure inevitably makes decrease the mark obtained by a thermodynamic model. This is simply because the success ratios are equal to 1 at the most.

3.2. Grading Results. Following the procedure described above, the final marks over 20 and the associated success ratios (see eq 34) for the *tc*-PR-Wilson, *tc*-PR-UNIQUAC, *tc*-PR-NRTL, and PR−Van Laar models are summarized in Table 2.

Remarks:

- At this step, it is worth recalling that in the paper by Jaubert et al.,[9] the PR−Van Laar model received a mark of 12.3/20. In this study, the mark reported in Table 2 is lower and only reaches 11.5/20. This is a simple consequence of the new grading procedure, which inevitably makes decrease the final mark by penalizing the presence of out-of-model data points.

- Similarly, in the paper by Nikolaidis et al.,[10] the PC-SAFT EoS with zero k_{ij} received a mark of 5.1/20. Once recalculated by considering success ratios lower than 1,

https://doi.org/10.1021/acs.iecr.1c03003
Ind. Eng. Chem. Res. 2021, 60, 17228−17247

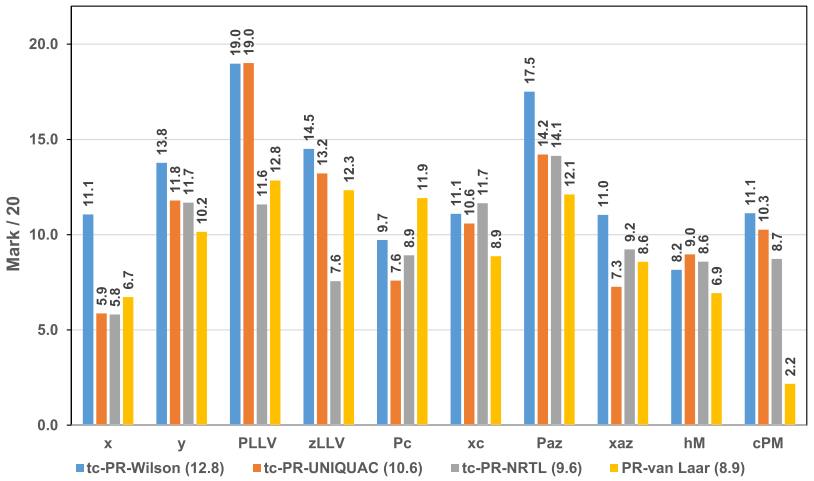

Figure 14. Overview of the accuracy of the *tc*-PR-Wilson, *tc*-PR-UNIQUAC, *tc*-PR-NRTL, and PR−Van Laar models by plotting the marks on 10 properties for the category including mixtures in which both cross- and self-associations take place (BACs 7−9).

as explained in this study, the mark should be slightly lower.

The detail of the calculated MAPEs, success ratios, and corresponding marks are reported in Tables 3 and 4 for *tc*-PR-Wilson, Tables 5 and 6 for *tc*-PR-UNIQUAC, Tables 7 and 8 for *tc*-PR-NRTL, and Tables 9 and 10 for PR−Van Laar.

The *tc*-PR-Wilson model takes the lead over the other models with a mark of 12.4/20. In terms of success ratio, the four models yield excellent overall success ratios since they are higher than 0.95. Differences between the studied models are observed for the success ratios of three-phase line and azeotropic point calculations. For both of them, it is observed that the *tc*-PR-Wilson model reaches the highest ratios. This is important from a qualitative standpoint because it means that this model is capable of predicting the right phase behavior topology for most of the binary systems present in the benchmark database.

From a quantitative standpoint, the overall marks per property are plotted in Figure 2. Such marks are calculated following eq 29, which is

$$\text{overall mark}_{\text{prop}} = \frac{1}{4} \times \left[\frac{\text{mark}^{\text{BAC}_1} + \text{mark}^{\text{BAC}_2} + \text{mark}^{\text{BAC}_3} + \text{mark}^{\text{BAC}_4}}{4} + \text{mark}^{\text{BAC}_5} + \text{mark}^{\text{BAC}_6} + \frac{\text{mark}^{\text{BAC}_7} + \text{mark}^{\text{BAC}_8} + \text{mark}^{\text{BAC}_9}}{3} \right] \quad (35)$$

It is possible to observe that the *tc*-PR-Wilson reaches the highest overall marks for liquid compositions, azeotropic pressures and compositions, three-phase pressures, and mixing heat capacities, which results in 5 out of 10 properties.

The PR−Van Laar model gives the best results for gas-phase compositions and critical pressures. In turn, three-phase compositions are similarly reproduced by the *tc*-PR-UNIQUAC, *tc*-PR-Wilson, and PR−Van Laar models. These properties are not reproduced accurately regardless of the investigated models. A similar trend is observed for critical compositions since all the *tc*-PR-$a_{\text{res}}^{\text{E},\gamma}$ model versions perform similarly by showing marks below 10/20.

In the next section, the discussion is focused on the performance of the investigated models in relation with the type of association exhibited by the binary systems.

3.3. Discussion. Among the nine BACs, the properties of mixtures from BAC 6 (HD + HA molecules that exhibit cross-association) are the most accurately predicted ones by the *tc*-PR-Wilson, *tc*-PR-UNIQUAC, and *tc*-PR-NRTL models with marks of 14.5/20, 16.0/20, and 15.5/20, respectively, while the PR−Van Laar model yields the highest performance for BAC 3 (HD + NA molecules), scoring a mark of 15.7/20. On the other hand, mixtures belonging to BAC 5, in which self-association takes place but tends to be broken, are represented unsatisfactorily by all the studied models.

In terms of the association degree (see Figure 3), the *tc*-PR-Wilson model performs better than the rest of the models for families where self-association is taking place (BAC 5 and BACs 7−9). In the case of systems that do not exhibit association (BACs 1−4), the PR−Van Laar model has the advantage. Finally, the *tc*-PR-UNIQUAC model best correlates the binary systems that exhibit cross-association (BAC 6).

In order to have a deeper insight, the marks over the 10 properties of interest are plotted for the four considered models. First, in Figure 4, for the category grouping BACs 1−4, it is possible to observe that the PR−Van Laar model yields higher marks for all the properties except for P_{LLV} and z_{LLV}. An important fact to be highlighted is the clear advantage for the PR−Van Laar model in the prediction of c_P^{M} data. This is illustrated in Figure 5 for the binary system cyclohexane + monochlorobenzene for which there is a huge difference between the calculated c_P^{M} with PR−Van Laar and the other three *tc*-PR-$a_{\text{res}}^{\text{E},\gamma}$ models. This led us to think that the difference in the temperature dependence of the Van Laar parameter with respect to those of the *tc*-PR-$a_{\text{res}}^{\text{E},\gamma}$ models, which are temperature-independent, could be the responsible for such results.

In addition, in Figure 6, it is possible to observe that the four models overestimate the critical pressures for the binary system nitrogen + *n*-pentane, but the PR−Van Laar model yields better results than *tc*-PR-$a_{\text{res}}^{\text{E},\gamma}$ models. Once again, the question of the temperature dependence of the parameters involved in the $a_{\text{res}}^{\text{E},\gamma}$ models arises. Indeed, as illustrated in Figure 6, the PR−Van Laar and *tc*-PR-NRTL models predict almost the same critical pressure at T = 398.3 K but at T = 447.9 K, the *tc*-PR-NRTL model presents some limitations to catch the right phase behavior.

https://doi.org/10.1021/acs.iecr.1c03003
Ind. Eng. Chem. Res. 2021, 60, 17228−17247

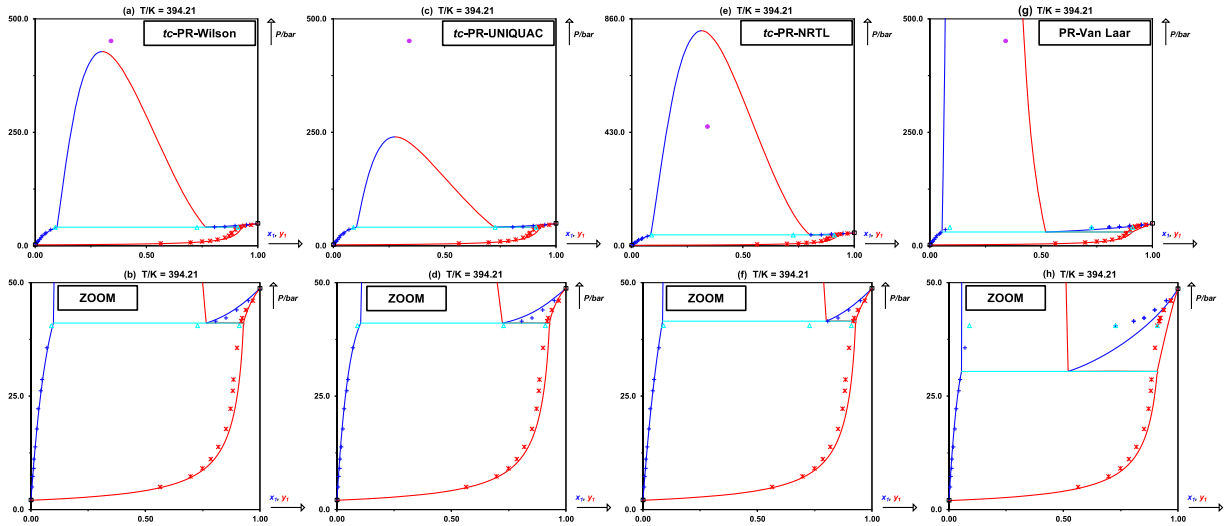

Figure 15. Pressure−composition VLE phase diagrams for the binary system dimethyl ether (1) + water calculated with the *tc*-PR-Wilson (a,b), *tc*-PR-UNIQUAC (c,d), *tc*-PR-NRTL (e,f), and PR−Van Laar (g,h) models. Phase equilibrium diagram convention: (red *): experimental dew points; bBlue +): experimental bubble points; (violet ○): experimental critical point; (teal ▲): experimental three-phase line compositions; (red −): calculated dew curve; (blue −): calculated bubble curve and; (teal −): calculated three-phase line.

Despite the limitations observed for some systems and illustrated in Figures 5 and 6, the *tc*-PR-$a_{res}^{E,\gamma}$ models are able to correlate with high accuracy the nonassociating binary systems. The binary system CH_4 + N_2 shown in Figure 7 perfectly demonstrates the strength of such models for these types of systems.

Considering now the category in which the systems exhibit cross-association (BAC 6), it should be noted that the four models perform very well, as shown in Figure 8. Most of the systems exhibit negative deviations from ideality so that the liquid phase does not tend to split. As a direct consequence, no three-phase VLLE data are available in this category. In particular, all the models equivalently correlate bubble and dew point compositions and critical pressures. In terms of azeotropic pressures, they are correlated with high accuracy (see Figure 8) by all the models with a slight disadvantage for the *tc*-PR-NRTL model. In turn, the *tc*-PR-UNIQUAC model reproduces critical compositions accurately, while the PR−Van Laar model seems to show some limitations compared to *tc*-PR-$a_{res}^{E,\gamma}$ models. Concerning h^M predictions, *tc*-PR-Wilson presents a clear disadvantage compared to the other models, which perform almost equivalently. Finally, once again, the PR−Van Laar model takes the lead on the correlation of c_P^M data, as observed with the binary system methyl acetate + chloroform presented in Figure 9.

As previously stated, binary systems belonging to BAC 6 are the ones most accurately correlated by the CEoS. Another representative example, exhibiting negative deviations from ideality and for which very negative h^M data are available, is shown in Figure 10.

The two remaining categories (BAC 5 and BACs 7−9) are those where at least self-association takes place. The first one, in which the self-association tends to be broken, gathers systems from BAC 5 only. The marks on the 10 properties of interest are plotted in Figure 11. They are the lowest in comparison to the other three categories, highlighting the difficulty of the CEoS to correlate systems that contain a self-associating compound such as water and a nonassociating component (e.g., a hydrocarbon). It is important to highlight that the *tc*-PR-Wilson model catches the right topology for almost all the systems of the considered BAC. For instance, in Figure 12, the pressure−composition VLE phase diagrams correlated by the four considered models for the binary system methanol + benzene are presented. It is possible to notice the clear difference between the diagram predicted by the *tc*-PR-Wilson model and the remaining ones. On this example, such an improvement on the diagram topology prediction entails a higher accuracy on azeotropic composition and pressure and, to a lesser extent, on bubble composition. The most visible effect of having the correct topology can be seen in Figure 12 on the h^M-composition diagrams. Indeed, all the models except the *tc*-PR-Wilson model predict a false LLE at 288.15 K and 1.0132 bar. As a direct consequence, the calculated h^M-composition diagrams exhibit a straight line between the compositions of the two liquid phases (from $x_1 \approx 0.25$ to $x_1 \approx 0.95$). The h^M-composition diagram calculated with the *tc*-PR-Wilson model has however the expected shape since such a model predicts a homogeneous liquid phase at 288.15 K and 1.0132 bar. A discussion around the shape of the h^M-composition diagram can be found in recently published papers.[32,33] For a system such as ethane + water (see Figure 13) that exhibits gas−gas equilibria and is thus a complex type III system in the classification scheme of van Konynenburg and Scott,[34,35] the *tc*-PR-Wilson model yields a success ratio of calculated over experimental critical points equal to 1; it however strongly overestimates critical pressures. The critical pressure overestimation is a consequence of the extreme steepness of the critical line that starts at the water critical point in a (P,T) projection. A temperature change of 2 K induces a change in the critical pressure of around 1000 bar.

Finally, the details of the behavior predictions of the binary systems belonging to BACs 7−9, that is, in which cross- and self-associations take place, are discussed (see Figure 14). First, the outstanding performances of the *tc*-PR-UNIQUAC and *tc*-PR-Wilson models regarding the prediction of the three-phase line pressures should be highlighted. They obtain a mark of 19/20 for such a property with a success ratio equal to 1. This is illustrated in Figure 15 with the binary system dimethyl ether + water. Another point to underline is the better accuracy on the bubble and dew compositions as well as on the azeotropic

https://doi.org/10.1021/acs.iecr.1c03003
Ind. Eng. Chem. Res. 2021, 60, 17228−17247

pressures obtained with the *tc*-PR-Wilson model with respect to the other models.

The analysis presented in this section makes it possible to conclude that the best choice to extend the *tc*-PR EoS to mixtures along with EoS/$a_{res}^{E,\gamma}$ MR is to use the residual part of the Wilson $a_{res}^{E,\gamma}$ model. Such a model, with a mark of 12.4/20, has the advantage over the other investigated models in this study. Moreover, it reaches a satisfactory overall success ratio of 0.96, meaning that this model is able to predict the existence of nearly all data points observed experimentally. The *tc*-PR-Wilson model distinguishes especially in the prediction of liquid- and gas-phase compositions, azeotropic points, and three-phase line pressures.

The weaknesses of the *tc*-PR-Wilson model are related to the reproduction of critical points, particularly for the systems in which self-association takes place (BAC 5 and BACs 7−9). In addition, the prediction of three-phase compositions needs to be improved for those systems that do not exhibit association or for which self-association tends to be broken. Finally, efforts are also required for improving the reproduction of caloric properties.

4. CONCLUSIONS

In the present work, the extension of the *tc*-PR EoS to mixtures has been investigated. For this purpose, EoS/$a_{res}^{E,\gamma}$ MRs derived by equaling the residual parts of the excess Helmholtz energy obtained from an EoS and from an explicit ACM such as Wilson, NRTL, and UNIQUAC were incorporated in the *tc*-PR EoS. The performance of the three resulting models was compared against the experimental data of the benchmark database, published by Jaubert et al.[9]

In light of the obtained results, it is possible to conclude that the best choice to extend the *tc*-PR EoS to mixtures along with EoS/$a_{res}^{E,\gamma}$ MRs is to use the residual part of the Wilson $a_{res}^{E,\gamma}$ model. The resulting model was named *tc*-PR-Wilson. This conclusion is supported by the fact that the *tc*-PR-Wilson model reaches the best results from the quantitative and qualitative standpoints. Nevertheless, improvements have to be made to better predict the behavior of systems in which hydrogen bonds are broken without the possibility to form new ones, as well as in the prediction of caloric properties for systems in which self-association does not take place.

The very good performances of the PR−Van Laar model (which is a nonpredictive version of the *E*-PPR78 model[36,37] relying on classical MRs with temperature-dependent BIPs $k_{ij}(T)$) should be acknowledged for its capacity to estimate caloric properties (h^M and c_P^M) more accurately than most of the other (more advanced) models and to reproduce phase diagrams of mixtures containing nonpolar and nonassociating compounds with a very reasonable accuracy.

The next step is to study the influence of the temperature dependence of the BIPs of the *tc*-PR-Wilson model on the reproduction of VLE, LLE, VLLE, and caloric property data. Next, the development of a group-contribution-based predictive *tc*-PR-Wilson model could be initiated.

ASSOCIATED CONTENT

Supporting Information

The Supporting Information is available free of charge at https://pubs.acs.org/doi/10.1021/acs.iecr.1c03003.

Derivation of MRs for a_m/b_m at infinite or zero pressure; combining rule for b_{ij}; and BIPs for the three *tc*-PR-$a_{res}^{E,\gamma}$ and PR−Van Laar models (PDF)

AUTHOR INFORMATION

Corresponding Authors

Romain Privat − *Université de Lorraine, École Nationale Supérieure des Industries Chimiques, Laboratoire Réactions et Géniedes Procédés (UMR CNRS 7274), 54000 Nancy, France;* orcid.org/0000-0001-6174-9160; Email: romain.privat@univ-lorraine.fr

Ioannis G. Economou − *Institute of Nanoscience and Nanotechnology, Molecular Thermodynamics and Modelling of Materials Laboratory, National Center for Scientific Research "Demokritos", GR-15310 Aghia Paraskevi, Greece; Chemical Engineering Program, Texas A&M University at Qatar, 23874 Doha, Qatar;* orcid.org/0000-0002-2409-6831; Email: i.economou@inn.demokritos.gr

Jean-Noël Jaubert − *Université de Lorraine, École Nationale Supérieure des Industries Chimiques, Laboratoire Réactions et Géniedes Procédés (UMR CNRS 7274), 54000 Nancy, France;* orcid.org/0000-0001-7831-5684; Email: jean-noel.jaubert@univ-lorraine1.fr

Authors

Andrés Piña-Martinez − *Université de Lorraine, École Nationale Supérieure des Industries Chimiques, Laboratoire Réactions et Géniedes Procédés (UMR CNRS 7274), 54000 Nancy, France*

Ilias K. Nikolaidis − *Institute of Nanoscience and Nanotechnology, Molecular Thermodynamics and Modelling of Materials Laboratory, National Center for Scientific Research "Demokritos", GR-15310 Aghia Paraskevi, Greece;* orcid.org/0000-0002-4816-4616

Complete contact information is available at: https://pubs.acs.org/10.1021/acs.iecr.1c03003

Notes

The authors declare no competing financial interest.

ACKNOWLEDGMENTS

The energy company TotalEnergies and more particularly Dr. Laurent Avaullée, Freddy Garcia, and Rémy Sancerry are gratefully acknowledged for sponsoring this research.

REFERENCES

(1) Le Guennec, Y.; Privat, R.; Jaubert, J.-N. Development of the Translated-Consistent *tc*-PR and *tc*-RK Cubic Equations of State for a Safe and Accurate Prediction of Volumetric, Energetic and Saturation Properties of Pure Compounds in the Sub- and Super-Critical Domains. *Fluid Phase Equilib.* **2016**, *429*, 301−312.

(2) Jaubert, J.-N.; Privat, R.; Le Guennec, Y.; Coniglio, L. Note on the Properties Altered by Application of a Péneloux−Type Volume Translation to an Equation of State. *Fluid Phase Equilib.* **2016**, *419*, 88−95.

(3) Privat, R.; Jaubert, J.-N.; Le Guennec, Y. Incorporation of a Volume Translation in an Equation of State for Fluid Mixtures: Which Combining Rule? Which Effect on Properties of Mixing? *Fluid Phase Equilib.* **2016**, *427*, 414−420.

(4) Le Guennec, Y.; Lasala, S.; Privat, R.; Jaubert, J.-N. A Consistency Test for Alpha-Functions of Cubic Equations of State. *Fluid Phase Equilib.* **2016**, *427*, 513−538.

(5) Le Guennec, Y.; Privat, R.; Lasala, S.; Jaubert, J.-N. On the Imperative Need to Use a Consistent α-Function for the Prediction of

Pure-Compound Supercritical Properties with a Cubic Equation of State. *Fluid Phase Equilib.* **2017**, *445*, 45−53.
(6) Twu, C. H.; Bluck, D.; Cunningham, J. R.; Coon, J. E. A Cubic Equation of State with a New Alpha Function and a New Mixing Rule. *Fluid Phase Equilib.* **1991**, *69*, 33−50.
(7) Pina-Martinez, A.; Le Guennec, Y.; Privat, R.; Jaubert, J.-N.; Mathias, P. M. Analysis of the Combinations of Property Data That Are Suitable for a Safe Estimation of Consistent Twu α-Function Parameters: Updated Parameter Values for the Translated-Consistent *tc*-PR and *tc*-RK Cubic Equations of State. *J. Chem. Eng. Data* **2018**, *63*, 3980−3988.
(8) Pina-Martinez, A.; Privat, R.; Jaubert, J.-N. Use of 300 000 Experimental Data over 1800 Pure Fluids to Assess the Performance of 4 CEoS: SRK, PR, tc-RK, tc-PR. *AIChE J.* **2021**, aic.17518. DOI: 10.1002/aic.17518.
(9) Jaubert, J.-N.; Le Guennec, Y.; Piña-Martinez, A.; Ramirez-Velez, N.; Lasala, S.; Schmid, B.; Nikolaidis, I. K.; Economou, I. G.; Privat, R. Benchmark Database Containing Binary-System-High-Quality-Certified Data for Cross-Comparing Thermodynamic Models and Assessing Their Accuracy. *Ind. Eng. Chem. Res.* **2020**, *59*, 14981−15027.
(10) Nikolaidis, I. K.; Privat, R.; Jaubert, J.-N.; Economou, I. G. Assessment of the Perturbed Chain-Statistical Associating Fluid Theory Equation of State against a Benchmark Database of High-Quality Binary-System Data. *Ind. Eng. Chem. Res.* **2021**, *60*, 8935−8946.
(11) Van der Waals, J. D.; Rowlinson, J. S. *On the Continuity of the Gaseous and Liquid States*, Dover phoenix editions; Dover Publications: Mineola, NY, 2004.
(12) Redlich, O.; Kwong, J. N. S. On the Thermodynamics of Solutions. V. An Equation of State. Fugacities of Gaseous Solutions. *Chem. Rev.* **1949**, *44*, 233−244.
(13) Peng, D.-Y.; Robinson, D. B. A New Two-Constant Equation of State. *Ind. Eng. Chem. Fundam.* **1976**, *15*, 59−64.
(14) Kontogeorgis, G. M.; Coutsikos, P. Thirty Years with EoS/g^E Models—What Have We Learned? *Ind. Eng. Chem. Res.* **2012**, *51*, 4119−4142.
(15) Huron, M.-J.; Vidal, J. New Mixing Rules in Simple Equations of State for Representing Vapour-Liquid Equilibria of Strongly Non-Ideal Mixtures. *Fluid Phase Equilib.* **1979**, *3*, 255−271.
(16) Michelsen, M. L. A Modified Huron-Vidal Mixing Rule for Cubic Equations of State. *Fluid Phase Equilib.* **1990**, *60*, 213−219.
(17) Michelsen, M. L. A Method for Incorporating Excess Gibbs Energy Models in Equations of State. *Fluid Phase Equilib.* **1990**, *60*, 47−58.
(18) Dahl, S.; Michelsen, M. L. High-Pressure Vapor-Liquid Equilibrium with a UNIFAC-Based Equation of State. *AIChE J.* **1990**, *36*, 1829−1836.
(19) Wong, D. S. H.; Sandler, S. I. A Theoretically Correct Mixing Rule for Cubic Equations of State. *AIChE J.* **1992**, *38*, 671−680.
(20) Jaubert, J.-N.; Privat, R. Cubic equations of state: what's new since Van der Waals? Which future?. *ESAT 2012 Plenary lecture*: Postdam, 2012;.
(21) Kontogeorgis, G. M.; Privat, R.; Jaubert, J.-N. Taking Another Look at the Van Der Waals Equation of State−Almost 150 Years Later. *J. Chem. Eng. Data* **2019**, *64*, 4619−4637.
(22) Jaubert, J.-N.; Privat, R. SAFT and Cubic EoS: Type of Deviation from Ideality Naturally Predicted in the Absence of BIPs. Application to the Modelling of Athermal Mixtures. *Fluid Phase Equilib.* **2021**, *533*, 112924.
(23) Kontogeorgis, G. M.; Folas, G. K. *Thermodynamic Models for Industrial Applications*; John Wiley & Sons, Ltd.: Chichester, U.K., 2010.
(24) Le Guennec, Y. Développement d'équations d'état Cubiques Adaptées à La Représentation de Mélanges Contenant Des Molécules Polaires (Eau, Alcools, Amines...) et Des Hydrocarbures. Ph.D. Thesis; Université de Lorraine, 2018.
(25) Wilson, G. M. Vapor-Liquid Equilibrium. XI. A New Expression for the Excess Free Energy of Mixing. *J. Am. Chem. Soc.* **1964**, *86*, 127−130.
(26) Smith, J. M.; Van Ness, H. C.; Abbott, M. M.; Swihart, M. T. *Introduction to Chemical Engineering Thermodynamics*, 8th ed.; McGraw-Hill Education: New York, NY, 2018.
(27) Tsuboka, T.; Katayama, T. Modified Wilson Equation for Vapor-Liquid and Liquid-Liquid Equilibria. *J. Chem. Eng. Jpn.* **1975**, *8*, 181−187.
(28) Abrams, D. S.; Prausnitz, J. M. Statistical Thermodynamics of Liquid Mixtures: A New Expression for the Excess Gibbs Energy of Partly or Completely Miscible Systems. *AIChE J.* **1975**, *21*, 116−128.
(29) Renon, H.; Prausnitz, J. M. Local Compositions in Thermodynamic Excess Functions for Liquid Mixtures. *AIChE J.* **1968**, *14*, 135−144.
(30) Jaubert, J.-N.; Privat, R. Relationship between the Binary Interaction Parameters (k_{ij}) of the Peng−Robinson and Those of the Soave−Redlich−Kwong Equations of State: Application to the Definition of the PR2SRK Model. *Fluid Phase Equilib.* **2010**, *295*, 26−37.
(31) Jaubert, J.-N.; Privat, R.; Mutelet, F. Predicting the Phase Equilibria of Synthetic Petroleum Fluids with the PPR78 Approach. *AIChE J.* **2010**, *56*, 3225−3235.
(32) Privat, R.; Jaubert, J.-N. Discussion around the Paradigm of Ideal Mixtures with Emphasis on the Definition of the Property Changes on Mixing. *Chem. Eng. Sci.* **2012**, *82*, 319−333.
(33) Qian, J.-W.; Privat, R.; Jaubert, J.-N.; Duchet-Suchaux, P. Enthalpy and Heat Capacity Changes on Mixing: Fundamental Aspects and Prediction by Means of the PPR78 Cubic Equation of State. *Energy Fuels* **2013**, *27*, 7150−7178.
(34) van Konynenburg, P. H.; Scott, R. L. Critical Lines and Phase Equilibria in Binary Van Der Waals Mixtures. *Philos. Trans. R. Soc., A* **1980**, *298*, 495−540.
(35) Privat, R.; Jaubert, J.-N. Classification of Global Fluid-Phase Equilibrium Behaviors in Binary Systems. *Chem. Eng. Res. Des.* **2013**, *91*, 1807−1839.
(36) Jaubert, J.-N.; Mutelet, F. VLE Predictions with the Peng-Robinson Equation of State and Temperature-Dependent k_{ij} Calculated through a Group Contribution Method. *Fluid Phase Equilib.* **2004**, *224*, 285−304.
(37) Xu, X.; Jaubert, J.-N.; Privat, R.; Arpentinier, P. Prediction of Thermodynamic Properties of Alkyne-Containing Mixtures with the *E*-PPR78 Model. *Ind. Eng. Chem. Res.* **2017**, *56*, 8143−8157.